Turbulence in the noise-producing region of a circular jet

By P. BRADSHAW, D. H. FERRISS AND R. F. JOHNSON
Aerodynamics Division, National Physical Laboratory, Teddington

(Received 13 June 1963 and in revised form 17 December 1963)

The flow in the noise-producing region of a circular jet is found to be dominated by a group of large eddies, containing nearly a quarter of the turbulent shear stress in the quasi-plane region of the shear layer: their contribution to the shear stress decreases as the effects of axisymmetry become noticeable at more than about two diameters downstream of the nozzle. These large eddies appear to be almost entirely responsible for the irrotational fluctuations near the nozzle, which, for this and other reasons, are larger relative to the reference dynamic pressure than in other shear flows. As a consequence of this, the convection velocity near the high- and low-velocity edges of the flow is biased towards the mean velocity in the high-intensity region. The dominance of the large eddies therefore explains the measurements of near-field pressure fluctuations by Franklin & Foxwell (1958), and of convection velocity by Davies, Barratt & Fisher (1963) and the present authors. The strength of these large eddies, compared with those in the boundary layer or wake, is remarkable.

The large eddies appear to be mixing-jets similar to those found by Grant (1958) in the wake, but with their projection in the (y, z)-plane inclined at about 45° to the y (radial) axis instead of lying along the y-axis as in the wake.

It is suggested that the augmentation of these large eddies by artificial means could be used to increase the mixing rate and permit the reduction of jet noise by means of acceptably short ejector shrouds.

The medium-scale motion is found to be far from isotropic in scales, although the two scales associated with a given *vorticity* component are more nearly equal. This phenomenon is also noticeable in the wake.

It is found that the departure from self-preservation, which starts when the shear layer thickness is no longer small compared with the nozzle radius, does not grossly affect the region of high turbulence intensity and maximum noise production until this region itself is no longer small compared with the radius. The maximum shear stress seven diameters downstream of the exit is still 70% of its value near the exit, and the non-dimensional mean velocity gradient is practically unchanged.

1. Introduction

Current studies of turbulent jet flows have been stimulated by the aircraft noise problem. Most of the noise generated by a circular jet exhausting into still air is found to be emitted within about ten nozzle diameters of the exit and several

model experiments on the turbulent flow in this region have been reported (Laurence 1956; Richards & Ffowcs Williams 1959; Davies *et al.* 1963). The flow in the noise-producing regions of a jet exhausting into a *moving* stream is almost the same at the airspeed ratios typical of aircraft on take-off or initial climb. In previous experiments, effort has been concentrated more on the quantities which are easiest to measure than those which throw direct light on the structure of the flow or the way in which it produces noise. The measurement of the fluctuating stress tensor which is the forcing term in Lighthill's (1952, 1954) equation for noise emission seems to be out of the question, and the development of approximations to it has not reached a state (Lilley 1958; Ffowcs Williams 1963) where reasonably simple measurements can be used to predict the noise output. In the absence of some technique for identifying or reducing only that very small part of the turbulence which produces the noise (and which is not necessarily associated with any particular group of eddies), the most promising method of achieving a worthwhile increase of noise reduction over that given by lobed nozzles seems to be the use of ejector shrouds surrounding the noise-producing region. Sufficiently long shrouds with walls of acoustically absorbent material would in principle produce a very great noise reduction, albeit with an unacceptable thrust and weight penalty. If shrouds are to be short enough to be operationally acceptable, they will have to be used with special nozzles or other devices to increase the rate at which the jet mixes with the surrounding air. It appears that progress with such nozzles will require a better understanding of the natural mixing processes, which must be based on more comprehensive measurements than have so far been made. The work reported here was undertaken for this reason.

A question of immediate interest was the existence or otherwise of a well-defined group of large eddies like those found in the wake and boundary layer by Grant (1958), which Townsend (1956) suggests will control the distortion of the boundary between the turbulent flow and the surrounding fluid, thus determining the rate of mixing. A broader aim was the collection of enough data on jet turbulence to bring our knowledge of this flow into line with our knowledge of the boundary layer and wake, which have been the subjects of most past experiments on turbulent shear flow. The first few sections of this paper give a general description of the flow, based on this data. This description also illustrates the dominance of the large eddies, which are discussed in detail in § 7.

The flow from a circular nozzle into still air can be divided into regions as shown in figure 1 (*a*). The transition region is usually small compared with the nozzle dimensions and is followed by a quasi-plane mixing layer in which the flow is self-preserving (Liepmann & Laufer 1947). In this region, velocity and intensity profiles are geometrically similar when plotted against $\eta \equiv (y-r_0)/x$ (see figure 1 (*a*) for notation). The present results were mostly obtained at $x/r_0 = 4$, but a scale of η is included on the graphs to permit comparison with other positions: see, for instance, figures 25–28. When the thickness of the mixing layer becomes an appreciable fraction of the nozzle radius, departures from self-preservation begin. At about four or five nozzle diameters downstream the shear layer has spread to the axis. At more than about 20 diameters downstream

another self-preserving state is reached: this asymptotic state, studied by Corrsin & Uberoi (1950, 1951), is usually called a 'jet' without qualification; here we shall use the term 'asymptotic jet'.

A review of the available information on plane mixing layers and asymptotic jets is given by Townsend (1956). It is clear, however, that most of the noise of circular jets is generated in the non-equilibrium region in which the flow characteristics change from those of a plane mixing layer to those of an asymptotic jet, so that these ideal flows are of interest chiefly as defining the limits between which the flow in the noise-producing region changes, but we shall see later that

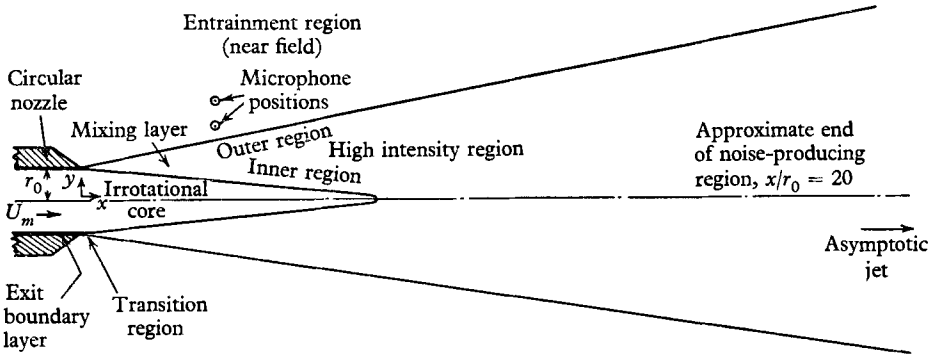

FIGURE 1 (*a*)

the flow properties in most of this region are roughly the same as in a plane mixing layer at the same distance from the exit. The final departure from this rough approximation, near $x/r_0 = 13$, is quite sudden (see figure 23) and the decrease in noise production is probably much more abrupt still so that the noise-producing region is very crudely a quasi-plane mixing layer terminated at $x/r_0 = 15$ or 20.

The rate at which the shear layer spreads at low Mach numbers is shown by the gas-injection schlieren pictures of plate 1, figure 1 (*b*) and (*c*). The vortex rings in the transition region, and the ensuing longitudinal striations predicted by Lin and Benney (Benney 1961) are visible. It should be noted that these pictures show the effect of refractive index (gas/air concentration ratio) changes *integrated* along the light path, and do not strictly represent a view of the laminar-turbulent interface.

2. Apparatus

A 2-in. diameter nozzle was chosen as being the largest for which noise measurements could be made on laboratory scale and which could be run from the existing compressed air supply: at low subsonic speeds, on the other hand, this is about the smallest nozzle capable of producing a fully developed turbulent mixing layer sufficiently close to the nozzle that the effects of transition and of axisymmetry do not overlap. A nominal Mach number of 0·3 was chosen, high enough for at least comparative noise measurements to be made but low enough for the effects of compressibility on the turbulent motion to be negligible.

Air was supplied from the 350 p.s.i. storage bottles through a remotely controlled silenced pressure reducer (Bradshaw 1963*a*), passed through a heater to raise its total temperature to that of the atmosphere so that the hot wires would not record temperature fluctuations, and delivered to the nozzle through a series of silencing baffles, a honeycomb, screens and a 36:1 contraction. The boundary layer at the nozzle exit was found to be laminar at $M = 0{\cdot}3$, with a displacement thickness of 0·008 in. and a shape parameter H of 2·2. Even a moderate increase of boundary-layer thickness, or a decrease in Mach number, leads to the onset of considerable 'scale effect', chiefly as a change in virtual origin of the mixing layer. (This may well be the explanation of the 'Mach number' effects found by some other workers but absent in the work of Maydew & Reed 1963, and casts some doubt on measurements with smaller jets than the present one.) Near $M = 0{\cdot}3$ and above, however, the present exit conditions are satisfactory, and a fair approach to similarity is attained in about one nozzle diameter, $U_m x/\nu \simeq 3{\cdot}5 \times 10^5$, which agrees with Liepmann & Laufer's figures. Checks have been made of the freedom from scale effect of the turbulence intensity and spectra in the fully developed turbulent flow.

Linearized constant-temperature anemometers were used, with wires of 0·00015 in. diameter about 0·02 in. long. The upper frequency limit of the anemometers depended on wire resistance and on airspeed but was usually about 40–50 kc/s (-3 dB) at the higher speeds. The multipliers, integrator and other processing apparatus used are described by Johnson (1962) and Bradshaw & Johnson (1963): the overall frequency response was in effect that of the anemometers.

All wires were calibrated in the centre of the jet and matched to the linearizing circuits. The X probes used to measured v- and w-component fluctuations were calibrated for yaw also, because of doubts about the relation between the geometrical angle of yaw of the wires and the 'effective' angle determining the yaw response.

3. The region of approximate similarity—general description

This is defined as the part of the jet which is little influenced either by the exit conditions or by axisymmetry: this is an elastic definition and we shall see that some of the gross properties of the flow are approximately similar up to seven or eight diameters from the exit. The equations of motion and continuity in a cylindrical mixing layer do not permit similar forms for the mean velocity and shear stress except very near the nozzle exit but in practice it seems that the first effect of axisymmetry is an inward displacement of the whole shear layer (figure 25) whose properties otherwise remain nearly the same as in the plane mixing layer.

The mean velocity (figure 2(*b*)) and shear stress (figure 3) profiles agree well with those of Liepmann & Laufer (1947). The mean velocity at $y/r_0 = 1$ or $\eta \equiv (y - r_0)/x = 0$, found to be $0{\cdot}69 U_m$ in the plane mixing layer, falls slightly with increasing x in the circular jet (figure 2(*a*)) and reaches $0{\cdot}65\, U_m$ at $x/r_0 = 4$. $\partial U/\partial y$ and the shear layer width remain closely the same as in the mixing layer. The u- and v-component turbulent intensities (figure 4) also agree quite well with

Liepmann & Laufer's measurements using non-linear constant-current hot wire apparatus. The w-component (figure 4) is found to be slightly larger than the v-component except near the inner edge of the flow where the v-component is bigger: measurements in the truly two dimensional mixing layer show that the v- and w-component intensities are almost identical except near the inner edge. The u-component is larger than the other two in the central region and reaches its maximum slightly further out, but is rather smaller near the inner edge.

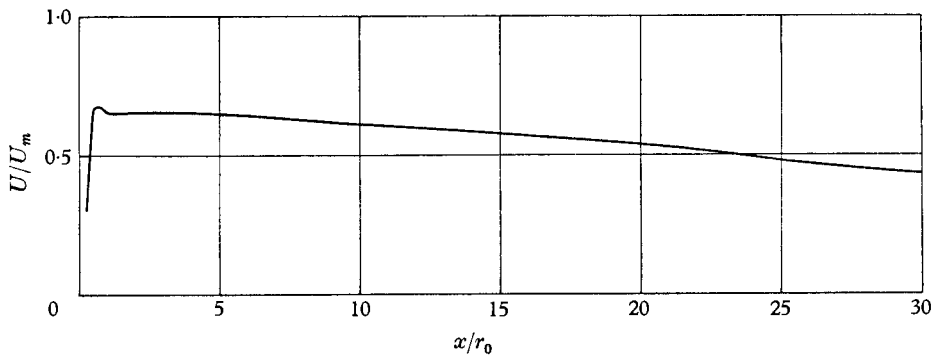

FIGURE 2(*a*). Mean velocity $y/r_0 = 1$ ($\eta = 0$).

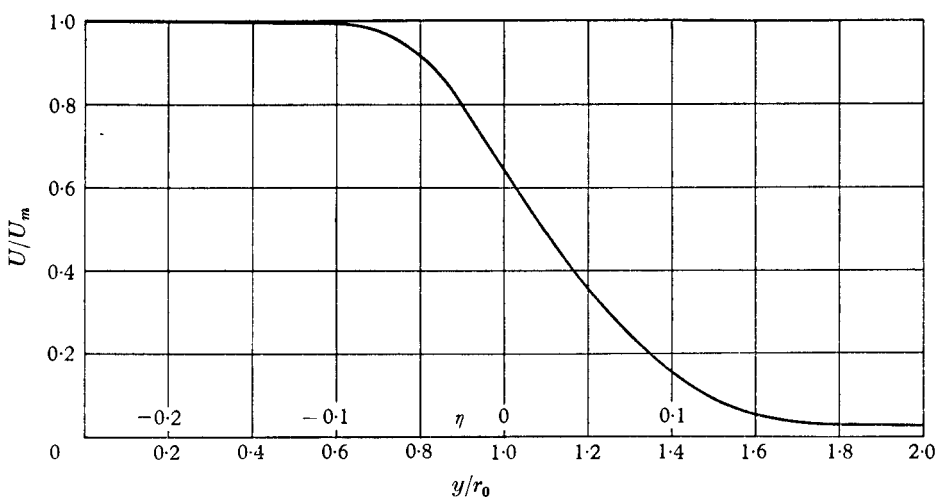

FIGURE 2(*b*). Mean velocity $x/r_0 = 4$.

Observation of oscilloscope traces shows that the v- and w-fluctuations near the inner edge consist of low-frequency undulations with occasional bursts of high frequencies, whereas the smaller u-component consists of occasional groups of negative-going spikes separated by intervals of near-quiescence: this indicates that the fluctuations in this region are partly due to the irrotational field of the more intense eddies which occur near $y/r_0 = 1$ and that the higher-frequency (vorticity-mode) fluctuations are caused by slower-moving patches of turbulent fluid which have erupted from nearer the centre of the shear layer.

Even in the high-intensity region, convection of fluid up and down the mean velocity gradient by the v-component, or 'shaking' of the shear layer to take another view, must contribute greatly to the u-component. This probably explains why the maximum intensity of the u-component occurs near the position of maximum mean velocity gradient whereas the v- and w-component maxima occur nearer the inner edge of the flow.

In the outer region the turbulence again becomes intermittent, and although the intensity falls rapidly the ratio of r.m.s. intensity to *local* velocity increases. Surprisingly, reversals of velocity direction do not seem to occur. The u-component vorticity-bearing fluctuations are now positive-going spikes but rotational fluid appears to penetrate further from the maximum intensity region than on the inner side of the flow, and consequently the irrotational field is not so obvious.

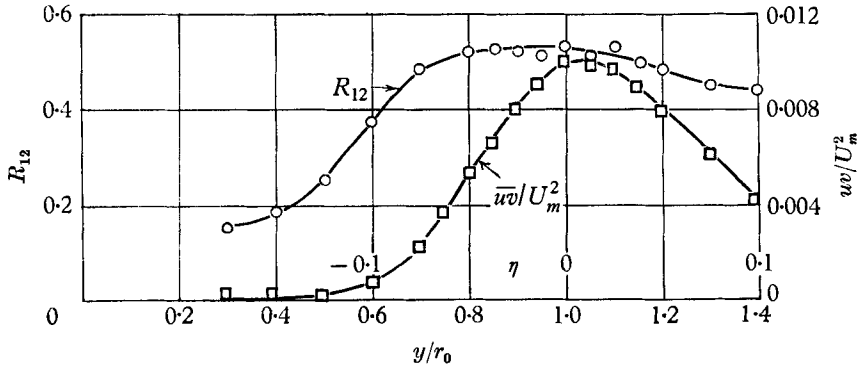

FIGURE 3. Turbulent shear stress and shear correlation coefficient · $x/r_0 = 4$.

The shear stress distribution (figure 3) is given both as $\overline{uv}/U_m^2$ and $\overline{uv}/\tilde{u}\tilde{v}$. (Here $\overline{F}$ is the time-mean, and $\tilde{F}$ the r.m.s. value, of F.) The latter expression is the shear correlation coefficient, $R_{12}(0,\ 0,\ 0:\ 0)$, which may be regarded as the efficiency of shear stress production by the turbulence, since it is the ratio of the actual shear stress to the shear stress that would be produced if the u- and v-component motions were perfectly correlated. It has a maximum value of $+0{\cdot}54$ (Liepmann & Laufer's value was 0·56) compared with about 0·5 in the boundary layer (Klebanoff 1955) and 0·44 in the asymptotic jet (Corrsin & Uberor 1951), and falls to zero at both edges of the flow because the u and v fluctuations become irrotational (the *turbulent* fluid near the edges may still have a finite value of R_{12}). It is reasonable that the mixing layer should have a higher value of shear correlation than the boundary layer or asymptotic jet: the boundary-layer flow is confined by a wall, so that any large-scale v-component motion must induce an inflow or outflow in the u- and w-component directions in order to maintain continuity, and this u- and w-component 'splashing' motion will not contribute to the shear stress: in the asymptotic jet negatively sheared fluid from the other side of the centre line will occasionally invade the flow. Since the maximum value of R_{12} is unity it is unlikely that the shear stress and mixing rate of any flow can be significantly increased without an artificial increase in

intensity levels. The maximum value of $\overline{uv}/U_m^2$ occurs at a small positive value of η, as required by the equation of motion.

The frequency spectra (figures 5–7) of the velocity components vary considerably across the jet. The spectral density ϕ per unit non-dimensional frequency $\omega x/U_m$ is normalized so that

$$\int_0^\infty \phi d(\omega x/U_m) = 1.$$

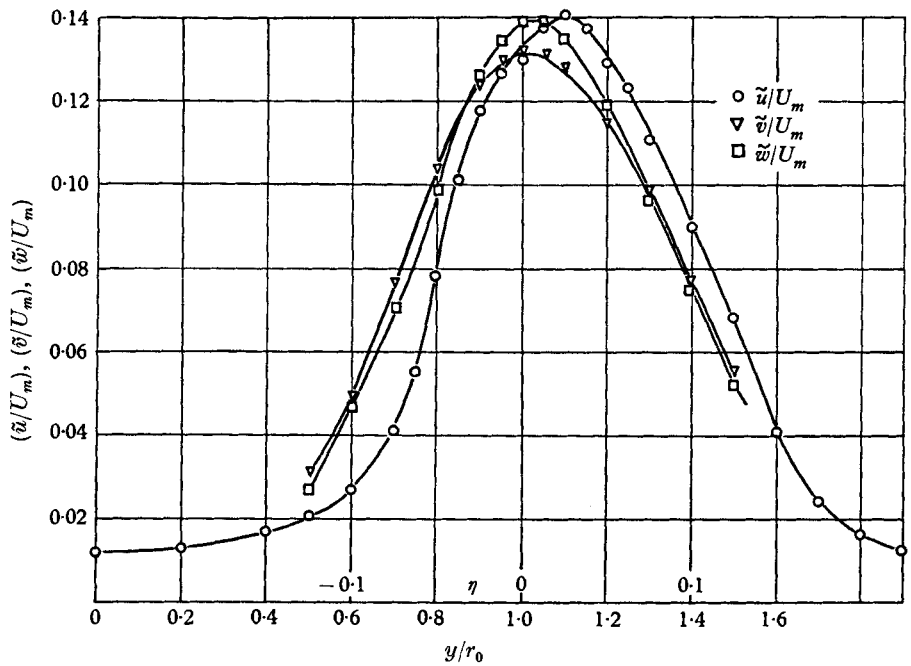

FIGURE 4. Root-mean-square turbulent intensities $x/r_0 = 4$.

In the inner region all three spectra have pronounced peaks, but in the region of maximum intensity the u-component spectrum peak disappears, and in the outer region all three spectra fall monotonically with increasing frequency. As Townsend (1958) has pointed out, correlations without negative loops (or, an approximate equivalent, spectra without peaks) correspond to decaying pulses of velocity, whereas peaked spectra obviously imply some sort of wave motion in a preferred frequency range but with no immediate indication of the number of wavelengths to which the motion extends. This supports the view that the flow in the outer region is made up of tongues of turbulent fluid which penetrate into the low-velocity region and are then re-entrained: we are not likely to learn very much about the high-intensity region by studying the properties of the outer region, with the possible exception of the intermittency.

The local isotropy hypothesis (Kolmogorov 1962) that the smaller eddies in the flow are unconscious of the preferred directions of the larger eddies is physically appealing and is a great help in inferring the properties of the high wave-number regions. One of the most easily checked predictions of the theory is that $\{\overline{u(\omega)\,v(\omega)}\}/\tilde{u}(\omega)\,\tilde{v}(\omega)\}$ tends to zero as $\omega \to \infty$ and several experimental

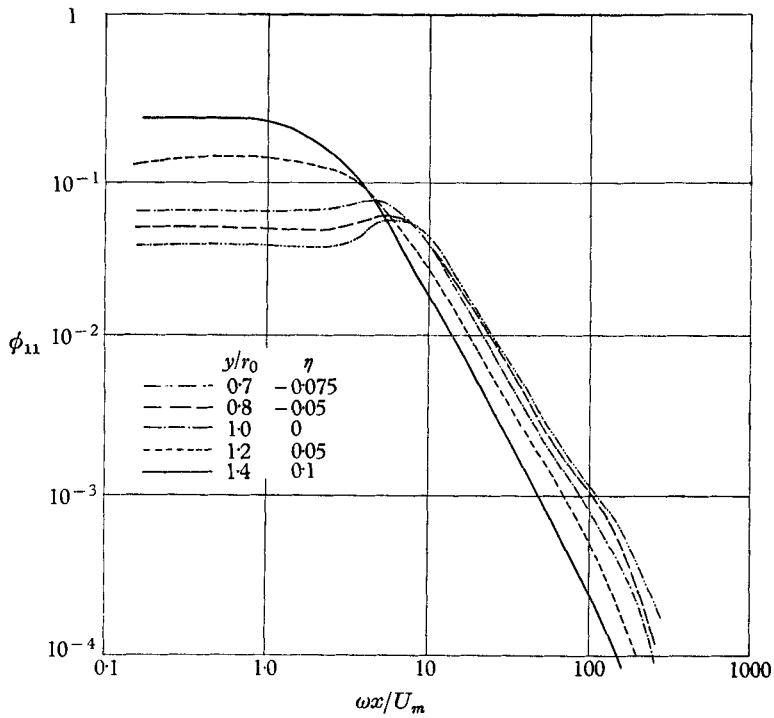

FIGURE 5. u-component spectra $x/r_0 = 4$.

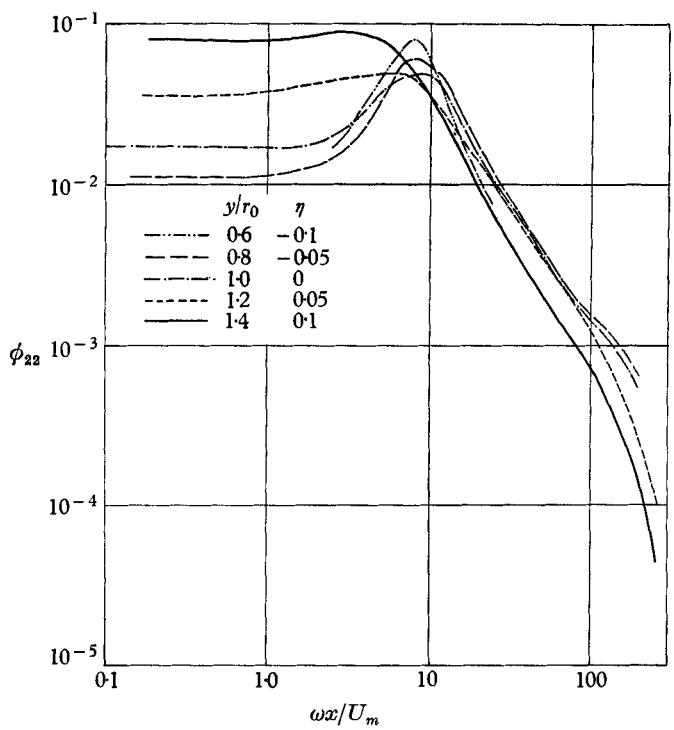

FIGURE 6. v-component spectra $x/r_0 = 4$.

demonstrations of its correctness have been given. The shear correlation spectra (figure 8) obtained in the present experiment do not reach zero within the frequency range of the equipment, the minimum values of $R_{12}(\omega)$ obtained being about 0·1 or 0·2, and eddy shedding from the prongs of the hot-wire probe causes the apparent correlation coefficient to rise again at the highest frequencies where the turbulent energy is very small. In view of the previous verifications of the prediction, however, it is reasonable to deduce that $R_{12}(\omega)$ does tend to zero

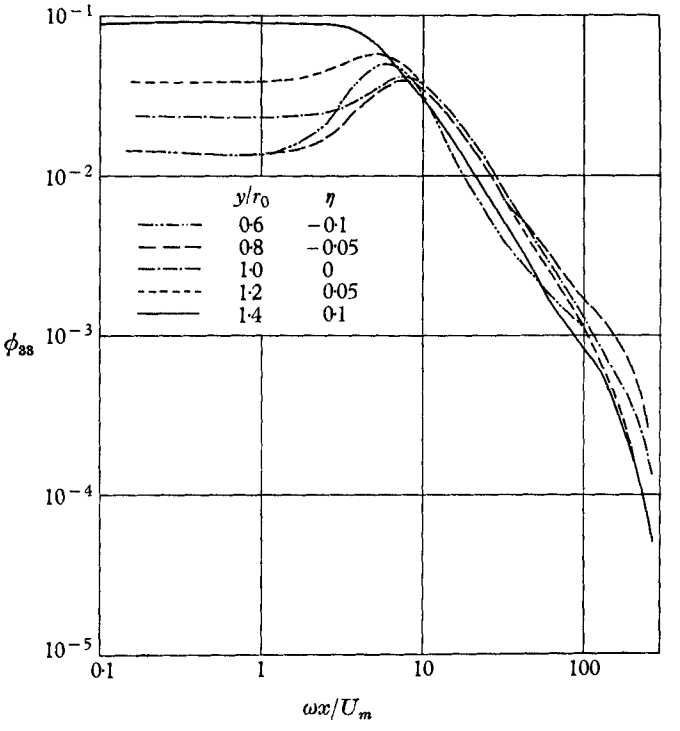

FIGURE 7. w-component spectra $x/r_0 = 4$.

in the jet. About 4 % of the energy in the ϕ_{12} spectrum at $y/r_0 = 1$ lies in the frequency range above $\omega x/U_m = 60$ compared with 10 % of the energy in the ϕ_{11} spectrum. Measurements of the spectral densities of the three velocity components at high frequencies showed that they were equal to within 20 % or so, but as the r.m.s. intensities are nearly equal anyway one would not really expect any great discrepancies: these are more likely to show up in transverse correlation measurements. The spectral densities of all three components at higher frequencies vary approximately as $\omega^{-\frac{5}{3}}$, which is another prediction of the local isotropy theory, but one doubts whether great significance attaches to this because the $\omega^{-\frac{5}{3}}$ variation begins at frequencies where $R_{12}(\omega)$ is still quite near its maximum value. Kistler & Vrebalovich (1961) seem to have found an $\omega^{-\frac{5}{3}}$ variation starting at surprisingly low frequencies in grid turbulence. A proper check of local isotropy in the mixing layer must await the measurement of the high-frequency spectra or correlations with small separation, but the

hypothesis clearly gives us no help in constructing a simplified model of the medium-scale energy-containing eddies.

The longitudinal correlations, $R_{ii}(r, 0, 0)$ (figures 9–11),* are similar in general shape to the autocorrelations or the Fourier transforms of the spectra: a closer comparison would reveal the departures from Taylor's (1938) hypothesis of rigid convection which will be discussed later (§ 5 (*b*)). The most interesting of

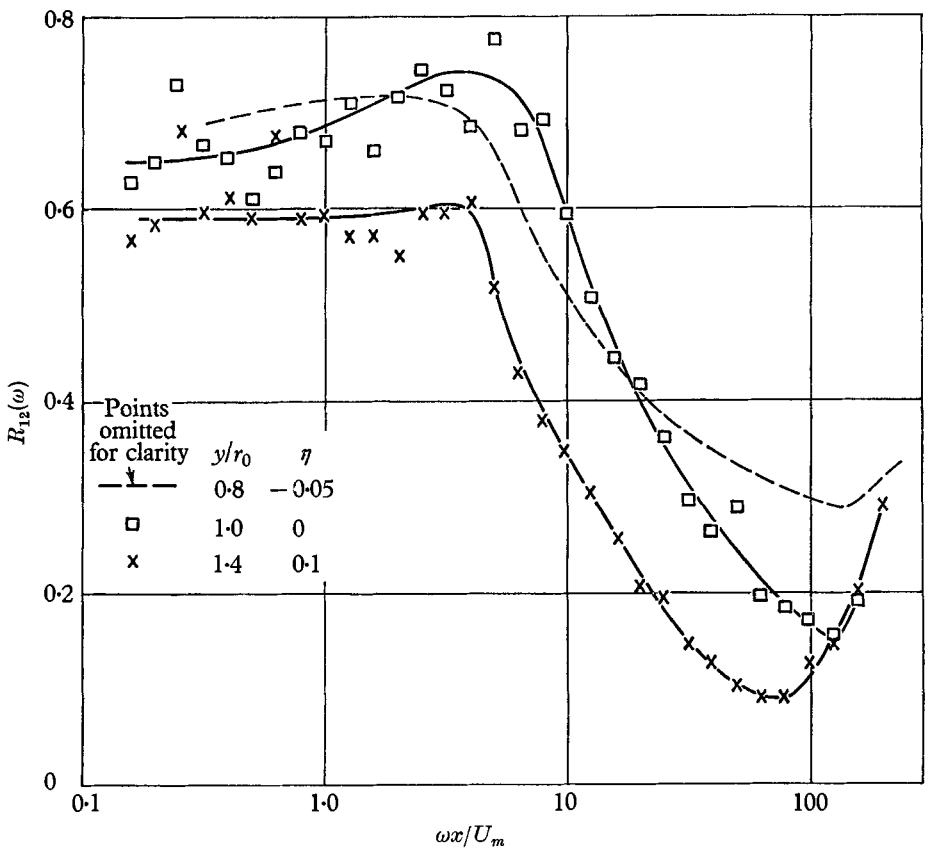

FIGURE 8. Correlation coefficient $R_{12}(\omega)$, $x/r_0 = 4$.

the correlations with radial separation (figures 12–14) are the $R_{22}(0, r, 0)$ and $R_{33}(0, r, 0)$ correlations, shown here as contour plots of correlation coefficient, $\overline{\{u_i(y)\, u_i(y+r)\}}/\{\tilde{u}_i(y)\, \tilde{u}_i(y+r)\}$. This type of plotting is more satisfactory for shear flows than the conventional plot of $\overline{\{u_i(y)\, u_i(y+r)\}}/\overline{u_i^2(y)}$ against r for each y, which would in this case give correlations exceeding unity because of the large intensity gradient. Also, a definition which is symmetrical in both space variables permits the correlations to be shown on contour plots, which is particularly useful for the $(0, r, 0)$ correlations. $R_{22}(0, r, 0)$ seems to take almost constant non-zero values near the edges, $R \to 0{\cdot}3$ at the inner edge and $R \to 0{\cdot}1$ at the outer edge. It should be noted that the analysis of Phillips (1955) shows that the $(0, r, 0)$

* Note that r denotes correlation separation (the usual notation): the nozzle radius is r_0. $(0, 0, r)$ denotes a separation r in the tangential direction.

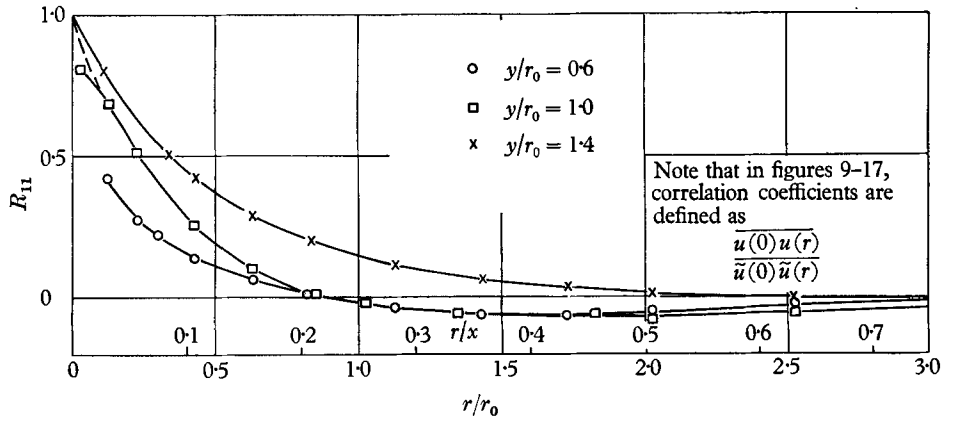

FIGURE 9. Correlation coefficient $R_{11}(r, 0, 0)$, $x/r_0 = 4$.

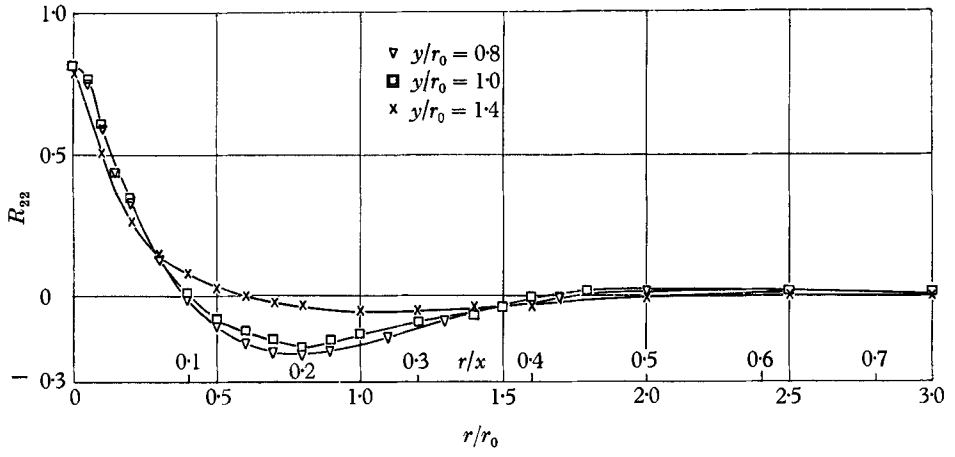

FIGURE 10. Correlation coefficient $R_{22}(r, 0, 0)$, $x/r_0 = 4$.

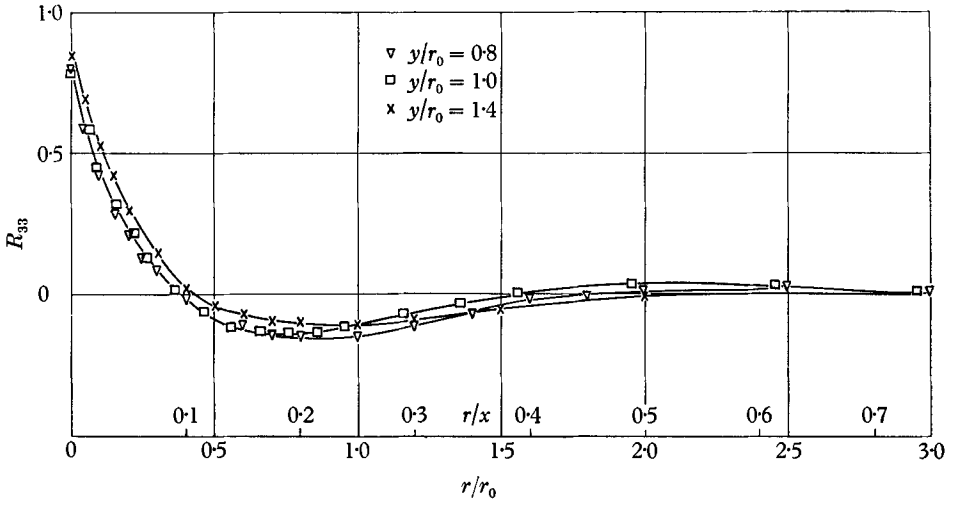

FIGURE 11. Correlation coefficient $R_{33}(r, 0, 0)$, $x/r_0 = 4$.

correlation coefficients outside a two-dimensional turbulent field eventually tend to zero as r^{-2}. The observed behaviour of $R_{22}(0, r, 0)$ confirms that the motion at the edges of the shear layer is largely that of the irrotational field induced by the high-intensity region, since Lilley & Hodgson (1960) show that the major term in the forcing function of the Poisson equation for the near-field pressure fluctuation is $(\partial v/\partial x)(\partial U/\partial y)$. We shall return to the correlation measurements in §7.

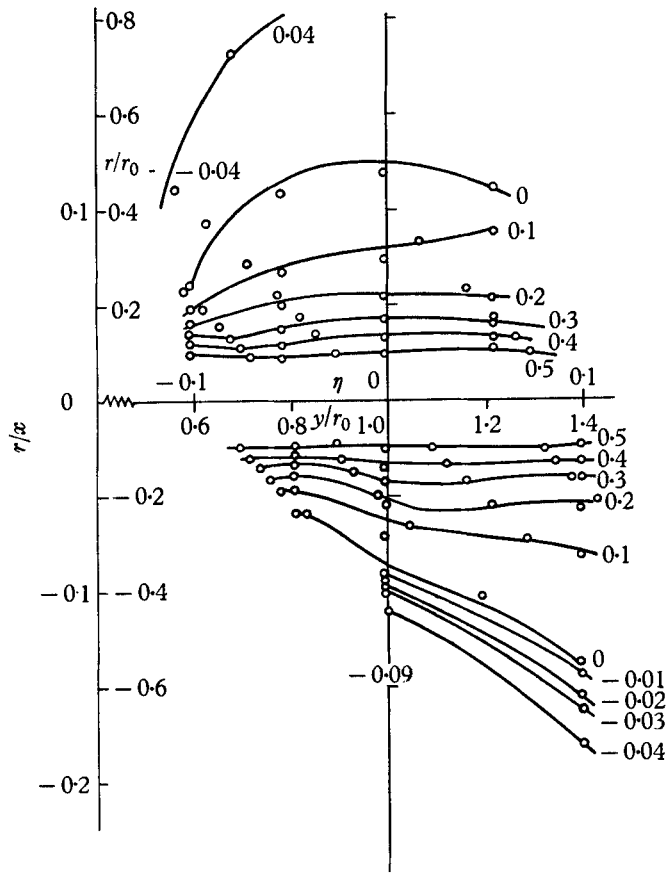

FIGURE 12. Correlation coefficient $R_{11}(0, r, 0)$, contours $x/r_0 = 4$.

4. The irrotational motion

(*a*) *In the jet core*

The reason for our interest in the irrotational field is that it is closely connected with the static pressure fluctuations in the central turbulent region, which cannot at present be directly measured but which are fundamental to the production of noise, and which also contribute to turbulent diffusion. Lighthill (1954) has shown that the largest contribution to $\partial^2 T_{ij}/\partial t^2$, which is one form of the 'forcing function' in the wave equation, in a low-speed flow with a large mean velocity gradient is $(\partial U/\partial y)(\partial p/\partial t)$. Lilley (1958) has obtained a possible approximate expression for this in terms of velocity fluctuations by the same method used to calculate the surface pressure fluctuations beneath a boundary layer, but direct

measurement would be very helpful. The nearest approach so far has been the study of the 'near-field' pressure fluctuations just outside the flow, by Franklin & Foxwell (1958), and others. These near-field fluctuations are important in their own right, because they can produce vibration (with consequent radiation of dipole noise) and structural damage in nearby parts of an aircraft structure, especially in ejector shrouds.

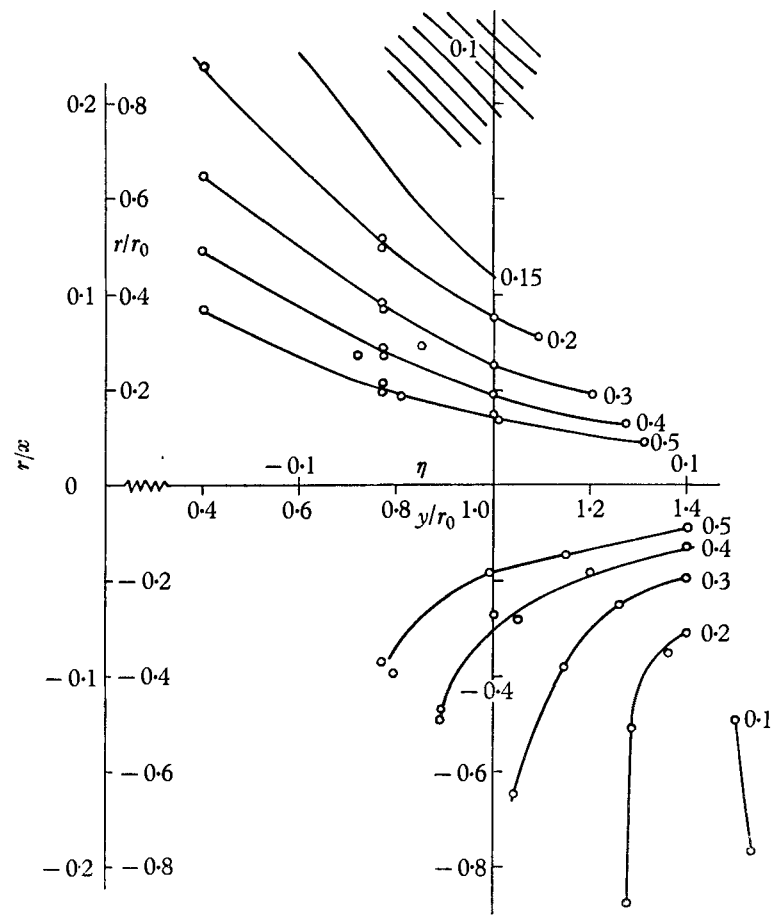

FIGURE 13. Correlation coefficient $R_{22}(0, r, 0)$, contours $x/r_0 = 4$.

The frequency spectra and correlations in the inner region, near $y/r_0 = 0{\cdot}6$ say, indicate that the irrotational field is composed chiefly of a small range of frequencies corresponding to the v- and w-component spectrum peaks in the high-intensity region near $y/r_0 = 1$. The fluctuations in the inner region are almost entirely confined to the v- and w-components which are nearly equal in conformity with the result of Phillips (1955) that in an irrotational random velocity field on one side of the plane $y = 0$, $\overline{v^2} = \overline{u^2} + \overline{w^2}$. At large y, $\overline{u^2}$ and $\overline{w^2}$ are expected to become equal. As mentioned above, the correlation coefficient between the v-component at $y/r_0 = 1$ and at positions in the irrotational core takes a nearly constant value of 0·3: correlations in narrow frequency bands

have not been made on the inner side of the layer, but it is certain that most of the contribution to this correlation coefficient comes from the spectral peak at $\omega x/U_m = 8$. The $R_{33}(0, r, 0)$ correlation coefficient between $y/r_0 = 1$ and positions in the core also appears to tend to a finite (positive) value.

The $R_{22}(0, 0, r)$ scale increases greatly at negative values of r but the $R_{33}(0, 0, r)$ scale is constant and roughly equal to the largest scale of $R_{22}(0, 0, r)$. The $R_{22}(0, 0, 0)$ and $R_{33}(r, 0, 0)$ scales are nearly equal, nearly constant, and rather

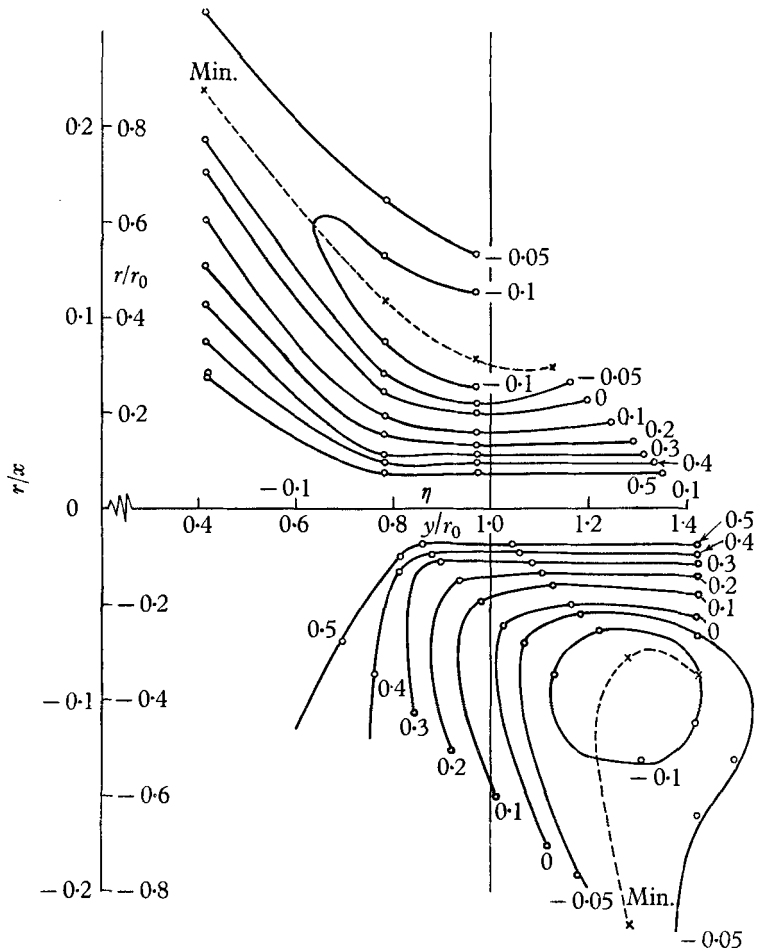

FIGURE 14. Correlation coefficient $R_{33}(0, r, 0)$, contours $x/r_0 = 4$.

larger than any value of the $(0, 0, r)$ correlation scales. We infer that the larger-scale turbulence in the high-intensity region, consisting of closely related v- and w-component wave motions, causes a v-component displacement flow in the inner irrotational region which spreads out in the z-direction, with an associated 'sloshing' of the w-component of approximately constant scale, and as a consequence the backflow takes place half a wavelength upstream and downstream.

As the maximum turbulent intensity in the mixing layer is much greater than in the wake or boundary layer, the absolute intensity in the irrotational field

is probably an order of magnitude greater, but the only directly relevant information is the observation by Lilley & Hodgson that the surface pressure fluctuation beneath a plane wall jet is about $0{\cdot}05(\frac{1}{2}\rho U^2)_{\max}$ compared with about $0{\cdot}005$ $(\frac{1}{2}\rho U^2)_{\max}$ beneath a boundary layer.

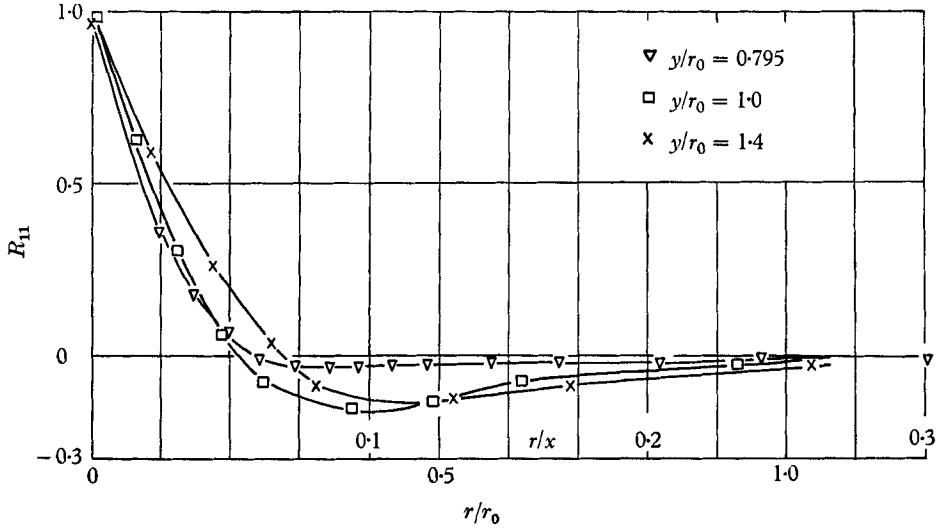

FIGURE 15. Correlation coefficient $R_{11}(0, 0, r)$ (circumferential traverse). $x/r_0 = 4$.

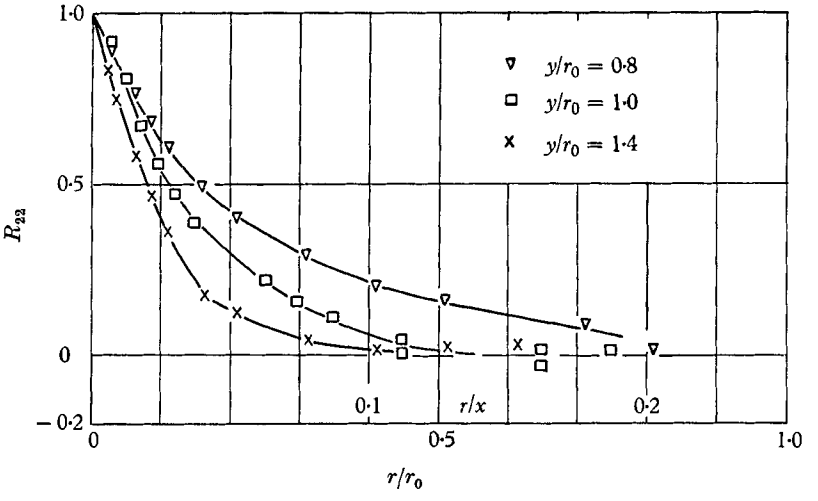

FIGURE 16. Correlation coefficient $R_{22}(0, 0, r)$, $x/r_0 = 4$.

(*b*) *In the near field*

As turbulent fluid seems to penetrate occasionally at least as far as $\eta = 0{\cdot}2$ it is necessary to make measurements of the irrotational flow at distances from the high-intensity region which are comparable with the predominant wavelengths of the high-intensity turbulence, so that there is a pronounced attenuation of the higher frequencies in the near-field spectra. According to Phillips's

(1955) analysis, in fact, the longitudinal wave-number spectrum of the near-field velocity fluctuation is

$$\phi(k_1) = \int \phi_{22}(k_1, k_3) \exp\left[-2\sqrt{(k_1^2+k_3^2)}\, x_2\right] dk_3,$$

where ϕ_{22} is a typical wave-number spectrum in the high-intensity region and x_2 is the distance between the high-intensity region and the point of observation in the near field. If the turbulence in the high-intensity region can be regarded

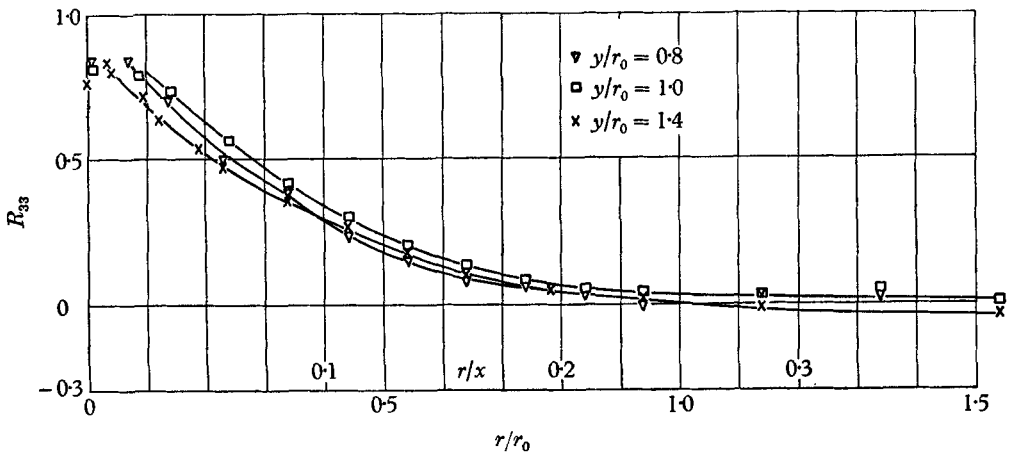

FIGURE 17. Correlation coefficient $R_{33}(0, 0, r)$, $x/r_0 = 4$.

as a rigid pattern convected at velocity U_c in the x_1-direction, the near-field pressure fluctuation spectrum is

$$\phi_p(k_1) = \rho^2 U_c^2 \int \frac{k_1^2}{k_1^2+k_3^2} \phi_{22}(k_1, k_3) \exp\left[-2\sqrt{(k_1^2+k_3^2)}\, x_2\right] dk_3,$$

so that at low k_1, $\phi_p \sim \omega^2$ at low ω (figure 18). At the larger distances x_2 from the high-intensity region, the $\exp[-2\sqrt{(k_1^2+k_3^2)}\, x_2]$ cut-off affects even the low-frequency portion of the spectrum: at $\eta = 0{\cdot}5$, $\phi_p \sim \omega^{1{\cdot}2}$ at low ω. This cut-off masks the predominance of the peak in the ϕ_{22} 'forcing' spectrum, but measurements of the correlation between the v-component fluctuation at $\eta = 0$ and the time derivative of the pressure fluctuation at $\eta = 0{\cdot}3$ show that the motion at the frequency of the peak is very highly correlated. The overall correlation coefficient is about 0·22 and the correlation coefficient in a one-third octave frequency band near $\omega x/U_m = 8$ is 0·59. The overall correlation coefficient between the v-component at $\eta = 0$ and the *velocity* fluctuation at $\eta = 0{\cdot}3$, measured with a linearized hot wire in the entrainment flow, is about 0·18 at $x/r_0 = 4$.

The spectrum of the velocity fluctuation at $\eta = 0{\cdot}3$ is shown in figure 19, plotted as $\log \phi_{22}$ against $\omega x/U_m$. The weighting factor $\exp[-2\omega x_2/U_c]$ is also shown: U_c was taken as $0{\cdot}65U_m$. It is seen that the spectrum falls slightly *less* rapidly than the weighting function in the mid-frequency range, but in view of our somewhat Procrustean adaptations of Phillips's idealized analysis this should not be taken too seriously. The spectrum flattens out appreciably at the highest frequencies. At about $\omega x/U_m = 30$ the signal became lost in amplifier noise but it seems that

the change in shape between $\omega x/U_m = 15$ and 25, where the signal-to-electrical-noise ratio is still adequately high, is real. The same effect is present in the pressure-fluctuation spectra (figure 18) being considerably more pronounced at

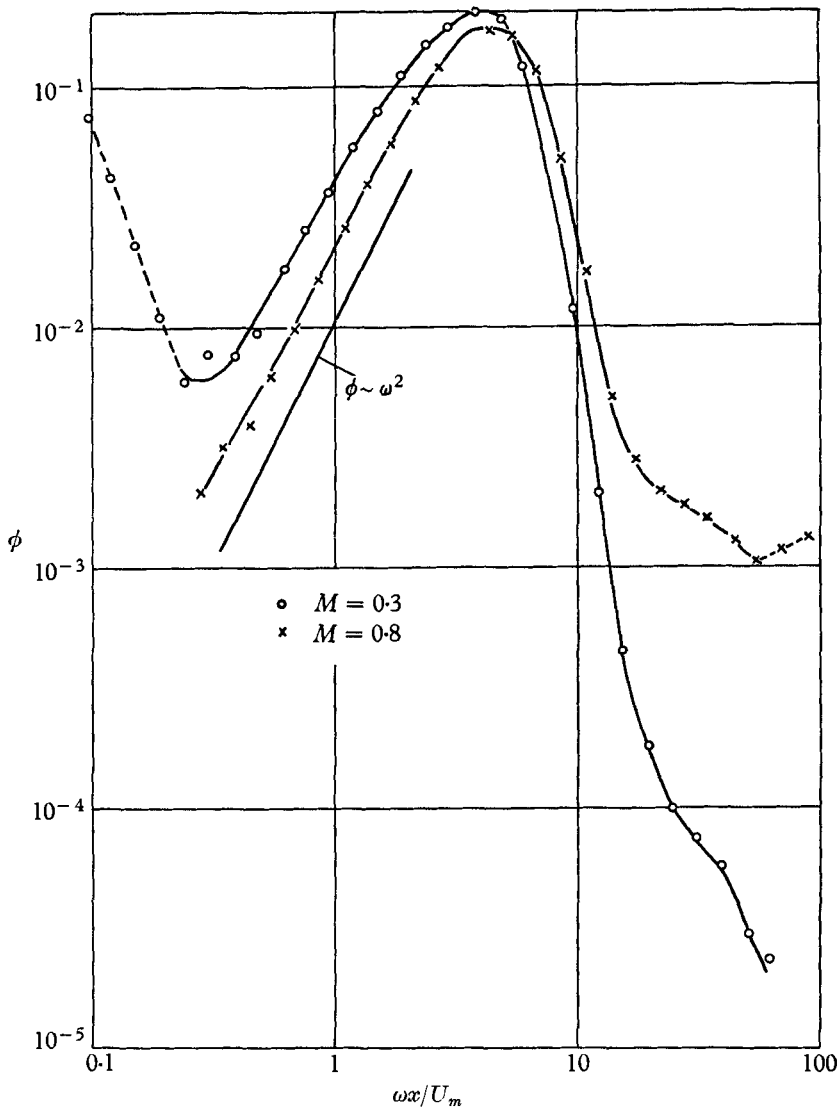

FIGURE 18. Near-field pressure spectra at $x/r_0 = 4$, $y/r_0 = 2{\cdot}25$ ($\eta \simeq 0{\cdot}3$).

$M = 0{\cdot}8$ than at $M = 0{\cdot}3$. It seems probable that radiated sound is responsible: the spectral density of the sound field varies roughly as M^7 whereas that of the near-field pressure varies as M^3. The ratio of the r.m.s. pressure fluctuation at $\eta = 0{\cdot}3$, say, to the dynamic pressure at the exit is likely to increase with Mach number for the additional reason that the weighting factor becomes

$$\exp\left[-2\sqrt{\{(k_1^2+k_3^2)(1-M_c^2)\}}\,x_2\right]$$

in compressible flow: the effect of the decrease in argument is noticeable in the

medium-frequency range of the pressure-fluctuation spectra, where the spectral density varies roughly as ω^{-6} at $M = 0{\cdot}3$ and ω^{-4} at $M = 0{\cdot}8$. Any decrease in turbulence intensity with increase in Mach number would oppose the observed increase in the pressure fluctuations.

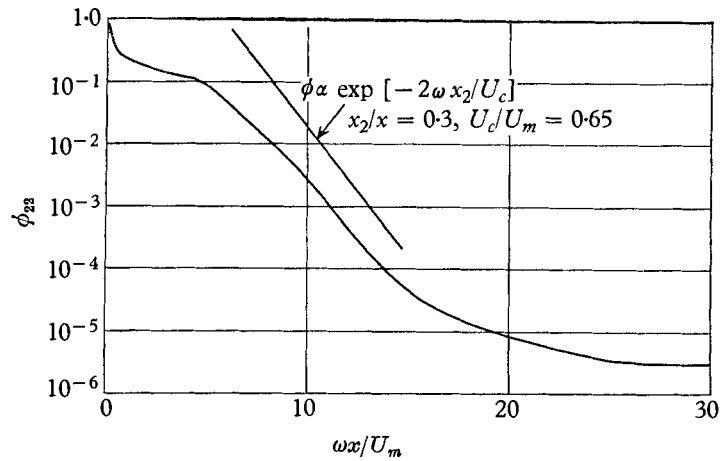

FIGURE 19. Near-field velocity spectrum $x/r_0 = 4$, $y/r_0 = 2{\cdot}25$.

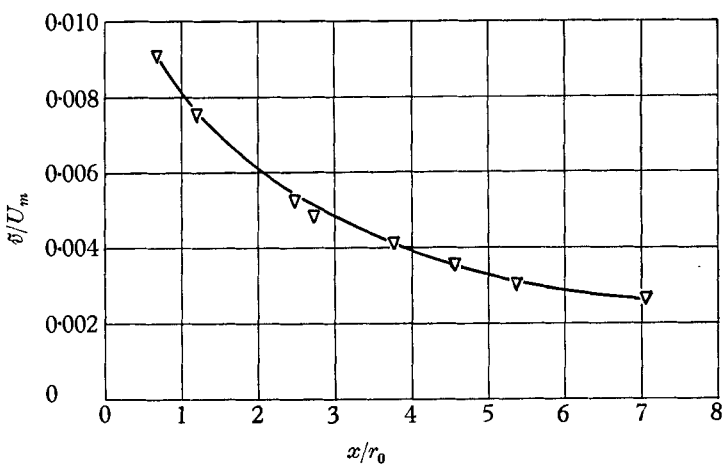

FIGURE 20. Near-field velocity fluctuation $\eta = 0{\cdot}3$.

At the the lowest frequencies both the velocity and pressure fluctuation spectra shown here rise abruptly with decreasing frequency. The velocity spectrum is affected by draughts in the entrainment region of the jet, whereas the crystal microphone signal is swamped by vibration and amplifier noise. Some spectra measured with a capacitor microphone of $\frac{1}{2}$in. diameter fell smoothly with decreasing frequency but are not presented here because the results at higher frequencies are expected to be in error owing to spatial resolution effects. These spectra may be found in Bradshaw (1963*b*), an investigation which shows the effect of the near-field pressure fluctuations in exciting organ-pipe resonances in ejector shrouds.

Further investigation of the near field as a means of inferring the properties of the turbulent flow is somewhat hampered by the very large departures from self-preservation of the circular jet at large positive η. The variation of the near-field velocity fluctuation at $\eta = 0{\cdot}3$ is shown in figure 20 (see also Möllo-Christensen 1963). The two-dimensional mixing layer would be a more useful flow for further study, though self-preservation is always restricted to $\eta \ll 1$ by the boundary-layer approximation.

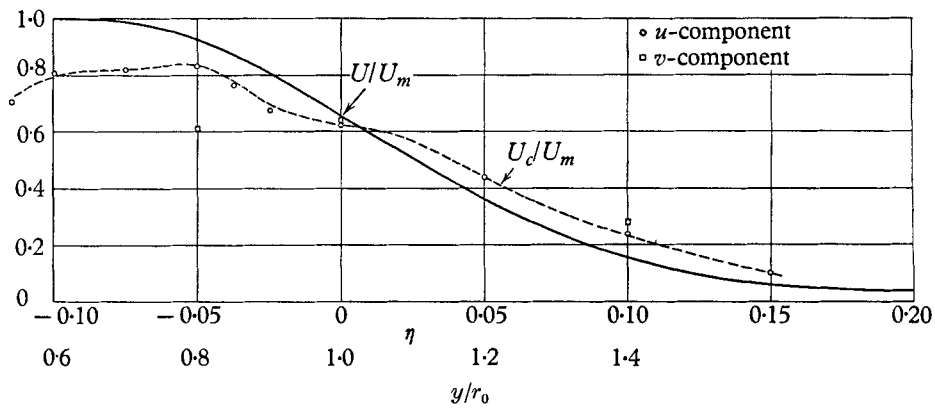

FIGURE 21. Convection velocity $x/r_0 = 4$.

(*c*) *The convection velocity*

The irrotational field seems to be largely responsible for the behaviour of the convection velocities of the u- and v-components which are compared with the mean velocity in figure 21: large differences occur in the intermittent regions near the edges of the shear layer. The convection velocity is defined here as the velocity of a frame of reference in which the time scale of the turbulence is a maximum, the most useful of the many possible definitions when noise production is being discussed. This velocity is the value of r/τ at which

$$\{\partial R(r, 0, 0; \tau)/\partial r\}_\tau = 0$$

and is found to be roughly constant over a range of values of τ. The difference between the convection velocity U_c and the mean velocity U in some parts of the flow has been reported by Davies (1963) who ascribes it wholly to the skewness of the velocity fluctuations in the intermittent region. This is not, however, large enough to explain the difference of 30 % between U_m and U_c at the inner edge of the shear layer where the fluctuation intensity is quite small, nor does it explain the differences between the convection velocities of the u- and v-components. The observations, and the observation of Franklin & Foxwell that the near-field pressure fluctuations are convected at about $0{\cdot}7U_m$ can be explained by noting that an irrotational field will move at the same speed as the eddies which give rise to it, in this case the eddies in the high-intensity region which move at about $0{\cdot}6U_m$. In the intermittent region on both sides of the shear layer the presence of vorticity fluctuations modifies the picture, as suggested by Davies, so that the u-component, which has a higher ratio of vorticity-mode to irrotational-mode

fluctuations than the v-component, has a convection velocity nearer to the mean velocity of the fluid.

These observations can, it should be observed, still be reconciled with the spirit of Taylor's original hypothesis that a turbulent eddy (meaning a patch of vorticity) remains associated with a given volume of fluid for most of its life. Turbulence may spread into initially irrotational fluid, and it now appears (Coles 1962) this process may be reversed in certain circumstances, possibly confined to transitional flows, but there is no reason to suppose a preferred direction of vorticity diffusion with respect to the *fluid*, except near the edges of the flow.

A comparison of the convection velocity in a jet with the values found by Favre, Gaviglio & Dumas (1957) in the boundary layer, where Taylor's hypothesis was more nearly obeyed, substantiates the suggestion that the irrotational field is proportionately stronger in the mixing layer than in other flows. The convection velocity results are reported in more detail in Wills (1963).

5. The medium-scale eddies

The space correlations of the three components at $y/r_0 = 1$ with separation in the y-direction are replotted in figure 22 as $R'_{ii} = \overline{\{u_i(0)\, u_i(r)\}}/\overline{u_i^2(0)}$, the more conventional definition, for direct comparison with the correlations with separations in the directions of approximate homogeneity, x and z. No attempt was made to measure v- and w-correlations above 0·8 or 0·9 because of limitations on wire length, probe proximity and frequency response. However, the measurements clearly show that the medium-scale structure of the flow is far from isotropic although the intensities are not too different. The non-dimensional separations r/x at which R'_{ii} has fallen to 0·5 arbitrarily taken as typical of the medium-scale motion, are

	$(r, 0, 0)$	$(0, r, 0)$	$(0, 0, r)$
R'_{11}	0·060	0·025	0·020
R'_{22}	0·032	0·040	0·030
R'_{33}	0·020	0·019	0·068

This table is roughly symmetrical about the leading diagonal, suggesting that the medium-scale flow would be better described in terms of the vorticity fluctuations, $R'_{22}(r, 0, 0)$ and $R'_{11}(0, r, 0)$, for instance, corresponding to the ζ-component of vorticity). A certain difficulty arises in defining the vorticity scale. The vorticity correlation is related to d^2R/dr^2 or the transform of $k^2\phi(k)$ so the integral scale is clearly zero. The first zero of the vorticity correlation occurs at $(dR/dr)_{\max}$ but this position is very ill-defined, and for practical purposes it is difficult to make a better choice of vorticity scale than the separation for which the velocity correlation takes an arbitrary value like 0·5. The r_i separations for a given value of R'_{ii} are naturally larger than the normal separations: the $R'_{11}(r, 0, 0)$ motion is always likely to be of larger scale than any other correlation since almost any conceivable eddy motion will contribute to it, either directly or through the amplifying effect of the mean-velocity gradient, and the $R_{33}(0, 0, r)$ motion is inherently unaffected by the velocity gradient and is therefore likely to spread unimpeded over large separations, but the $R_{22}(0, r, 0)$ scale is barely

larger than the other R'_{22} scales. We see that the $R'_{ii} = 0{\cdot}5$ scales associated with the vorticity components ξ, η and ζ are

$$\xi\text{: } 0{\cdot}019 \text{ to } 0{\cdot}030, \quad \eta\text{: } 0{\cdot}02 \quad \text{and} \quad \zeta\text{: } 0{\cdot}025 \text{ to } 0{\cdot}032.$$

As the shear stress $-\rho\overline{uv}$ is produced by the stretching of vortices with roughly equal ξ and η components one expects these two scales to be smaller than that of ζ, but the difference is barely significant. The corresponding separations in the boundary layer at $y/\delta_0 = 0{\cdot}66$ and in the wake at $y/l_0 = 1{\cdot}8$ (Grant 1958) are respectively

$(r/\delta_0) =$				and	$(r/l_0) =$		
	0·13	0·13	0·13		3·7	3·0	2·2
	0·10	0·11	0·09		2·6	1·6	1·4
	0·09	0·04	0·16		2	1·3	2·4

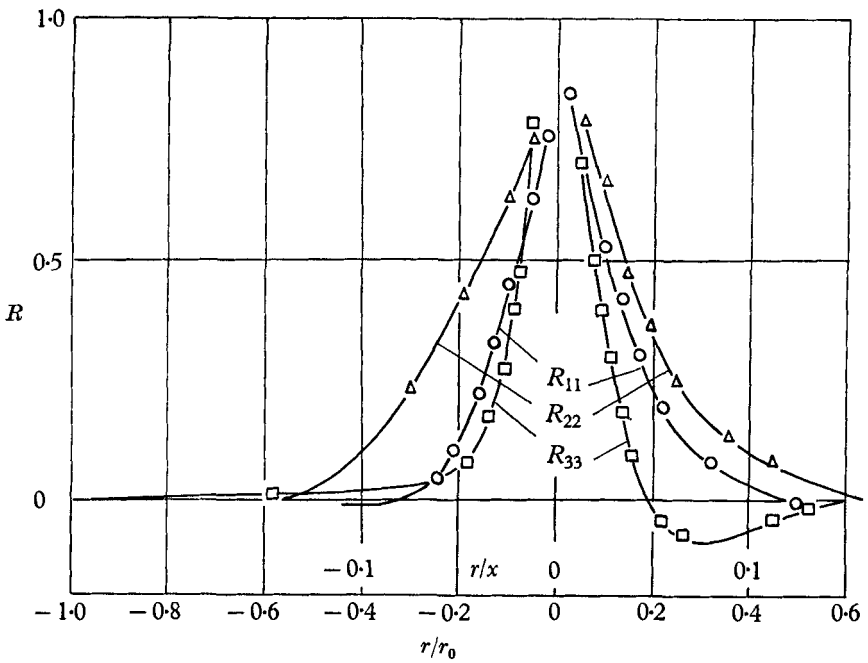

FIGURE 22. $R_{ii}(0, r, 0)$, $x/r_0 = 4$, $y/r_0 = 1$, $\eta = 0$.
Correlation normalized by intensity at $\eta = 0$.

where δ_0 is the distance from the surface at which the velocity in the boundary layer is $u_\tau = \sqrt{(\tau_w/\rho)}$ below the free-stream velocity and l_0 is the distance from the centre line at which the velocity defect in the wake is $e^{-\frac{1}{2}}$ (= 0·606) of its maximum value. The wake results in particular show the skew-symmetry effect, with $R'_{ii} = 0{\cdot}5$ at

$$\xi\text{: } 1{\cdot}3 \text{ to } 1{\cdot}4, \quad \eta\text{: } 2{\cdot}0 \text{ to } 2{\cdot}2, \quad \zeta\text{: } 2{\cdot}6 \text{ to } 3{\cdot}0.$$

The integral scales $\int_0^\infty R'dr/x$ at $y/r_0 = 1$, measured at $x/r_0 = 4$, are

	$(r, 0, 0)$	$(0, +r, 0)$	$(0, -r, 0)$	$(0, 0, r)$
R'_{11}	0·0445	0·033	0·024	0·0065
R'_{22}	0·015	0·044	0·048	0·038
R'_{33}	0·012	0·016	0·024	0·087

The percentage accuracy of the $R_{22}(r, 0, 0)$ and $R_{33}(r, 0, 0)$ scales is likely to be poor as they represent the small difference between two large quantities. In fact, a scale corresponding to the maximum spectral density would be generally more informative than the integral scale, which corresponds to the spectral density at zero wave-number.

6. Departures from similarity: the effects of axisymmetry

Since most of the turbulent energy in the mixing layer resides quite near $y/r_0 = 1$ or $\eta = 0$ (two-thirds of $\int q^2 dy$ lying between $\eta = +0{\cdot}05$ and $-0{\cdot}05$) it is likely, and indeed it is found that the flow in this region will be largely unaffected by axisymmetry until the width of the high-intensity region (rather than the *total* width of the shear layer) becomes comparable with the nozzle radius, even though the flow outside the high intensity region may be greatly altered. We now proceed to examine the departures from similarity in the region near the end of the irrotational core.

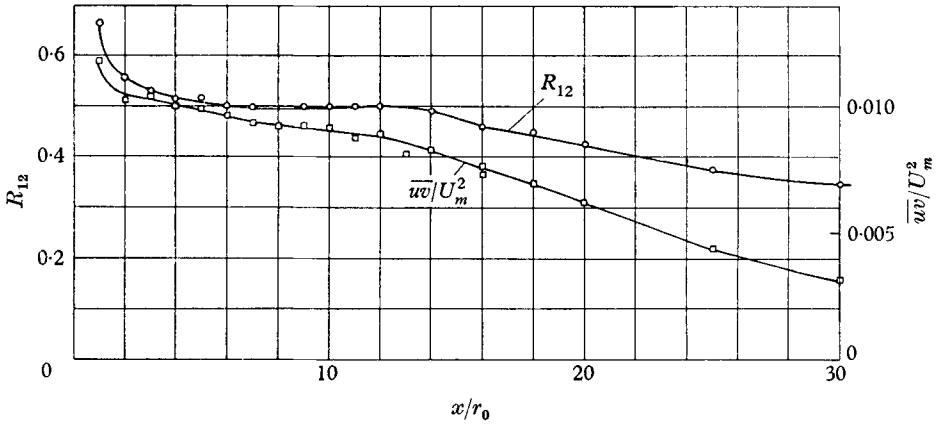

FIGURE 23. Turbulent shear stress and shear correlation coefficient $y/r_0 = 1$.

The approximation to similarity becomes less accurate for $x/r_0 > 4$: in fact quantities like the mean velocity (figure 2 (*a*)), shear stress and shear correlation coefficient (figure 23), measured at $y/r_0 = 1$, decrease continuously from very near the nozzle exit. The mean velocity at $y/r_0 = 1$ is nearly $(0{\cdot}68 - 0{\cdot}007x/r_0)\, U_m$ for $3 < (x/r_0) < 20$. The v- and w-component intensities (figure 24) also decrease, but the decrease in u-component is barely noticeable until $x/r_0 \sim 8$, partly because the whole shear layer is shifted in the η-direction and the u-component in the mixing layer reaches a maximum at a small positive value of η. Figures 25–28 show the velocity, shear stress and intensity profiles at $x/r_0 = 8$ and $x/r_0 = 15$. The intensities on the axis are shown in figure 29. The v-component spectrum peak (figure 30) disappears completely by $x/r_0 = 8$. This seems to be a real effect and not a mere swamping of the eddies which contribute to the peak by increased contributions to the low frequencies from other parts of the circumference: the normalized spectral density at low frequency is constant until

$x/r_0 = 4$ and only rises 35 % by $x/r_0 = 8$. In view of the checks on Reynolds number similarity mentioned in § 2, scale effect can almost certainly be ruled out. The w-component spectrum in the jet (figure 31) is more accurately self-preserving and the peak is still noticeable at $x/r_0 = 15$ but it is clear that the large eddies are greatly modified as the flow changes from a quasi-plane mixing layer to an axisymmetric jet.

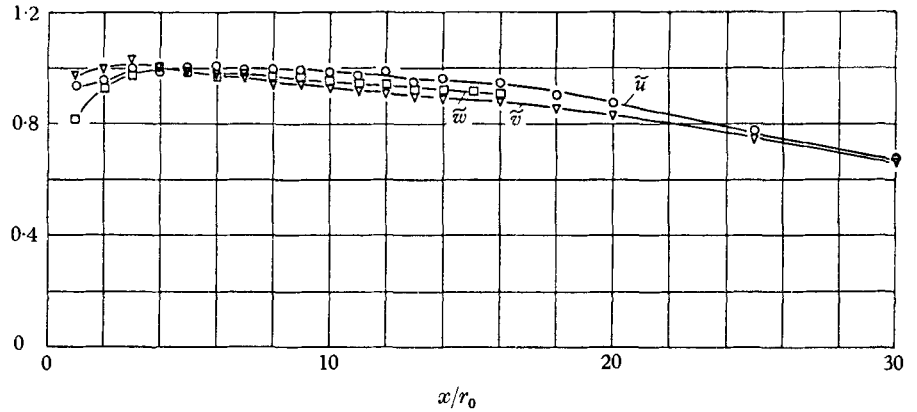

FIGURE 24. Root-mean-square turbulent intensity components at $y/r_0 = 1$ normalized by the values at $x/r_0 = 4$.

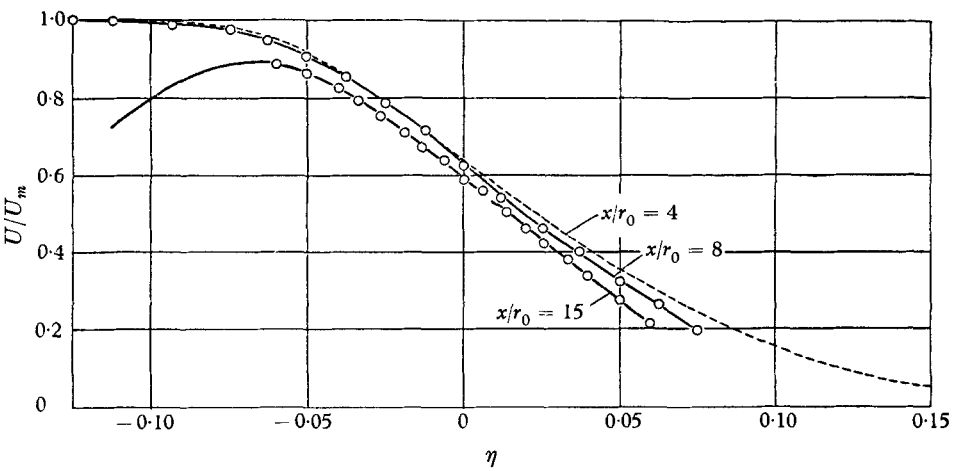

FIGURE 25. Mean velocity $x/r_0 = 4$, 8 and 15, to the same scale of η.

7. The large eddy distribution

Townsend's hypothesis (1956, 1958: see also Grant 1958) is that the correlations at large separations are determined by a well-defined but fairly weak group of large eddies, an order of magnitude larger than the eddies containing most of the turbulent energy, which gain energy from the mean flow during the middle 'equilibrium' period of their lives at approximately the same rate at which they lose energy to the smaller-scale motion, and which are chiefly responsible for distorting the boundary of the rotational fluid, thus controlling the rate of spread-

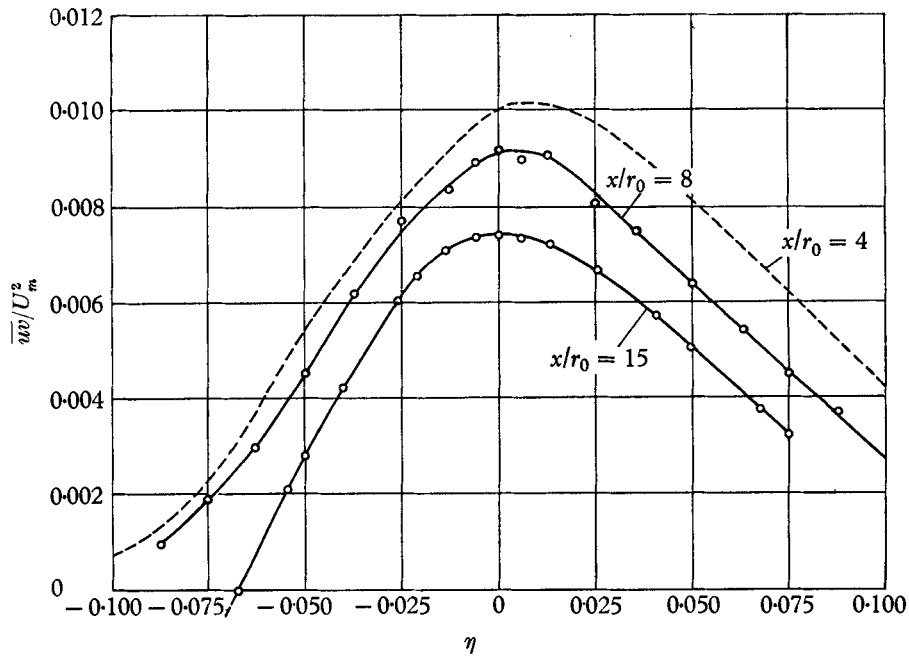

FIGURE 26. Turbulent shear stress $x/r_0 = 4$, 8 and 15 to the same scale of η.

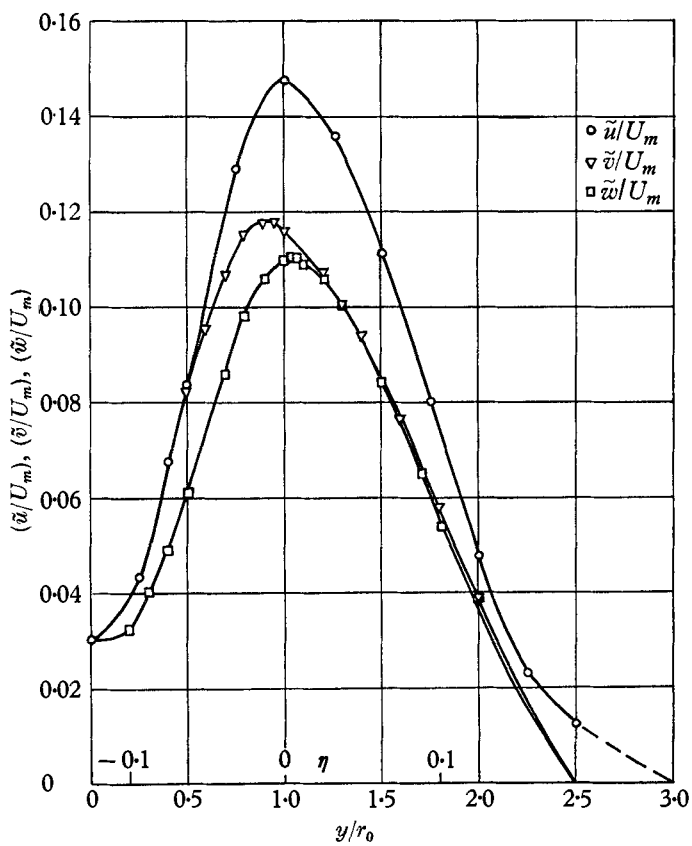

FIGURE 27. Root-mean-square turbulent intensities $x/r_0 = 8$.

ing of the flow. Townsend goes on to deduce a relation between the mean velocity distribution and the Reynolds shear stress from the equilibrium condition for a possible eddy shape. Grant (1958) has measured spatial correlations in the wake and boundary layer and deduced eddy shapes which fit these correlations.

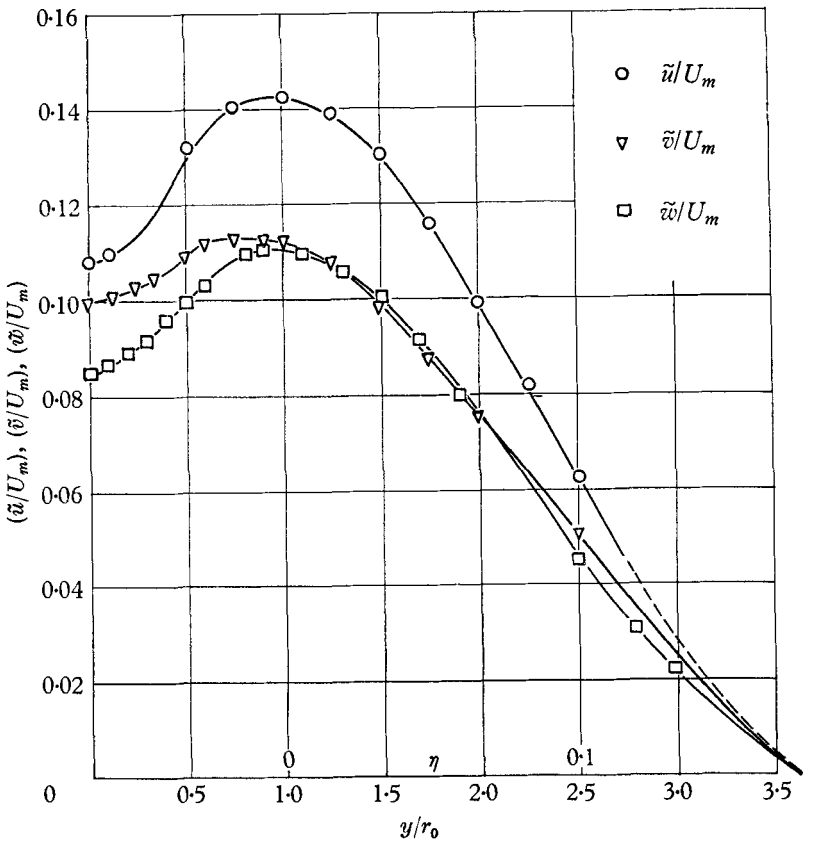

FIGURE 28. Root-mean-square turbulent intensities $x/r_0 = 15$.

The large eddy may be regarded as the type of finite-amplitude disturbance to which the turbulent flow is least stable. Too close a parallel with laminar-flow stability should not be assumed, and the stability theory for finite disturbances has not progressed far enough to indicate possible forms for self-limiting disturbances in a laminar flow except for the special case of flow between rotating cylinders: in free shear layers or boundary layers the finite-amplitude disturbances tend to become three-dimensional (Benney 1961; Klebanoff, Tidstrom & Sargent 1962) (see figure 1 (*b*)). If the large eddy is the least-stable disturbance, it is presumably the one which can be artificially augmented with the least expenditure of energy. Townsend's hypothesis implies that this augmentation would be the most efficient way of increasing the Reynolds shear stress and the mixing rate, and this is the reason for our present interest. Before the measurements were started, it was assumed that the large eddies would, as postulated by Townsend, have a fairly low intensity and large wavelength, and therefore contribute

little to the pressure fluctuations and noise output, so that augmenting them would not affect the noise output other than through their effect on the smaller-scale turbulence. However, if we take the spectrum of the large eddy motion to be represented by the difference between the actual shear stress spectrum $R_{12}(\omega)\{\phi_{11}(\omega)\,\phi_{22}(\omega)\}^{\frac{1}{2}}$, which has a large peak near $\omega x/U_m = 8$, and a plausible unpeaked spectrum with the same behaviour far from the peak, we see that the large eddy motion contributes something like a quarter of the total shear stress. Although these strong, large eddies undoubtedly control the flow as Townsend suggests, it is likely that Townsend's 'equilibrium' hypothesis is only applicable to weak eddies. Since the large eddies have a disproportionately long life, we may assume that their contribution to the noise output is less than that of an equally intense distribution of, say, isotropic turbulence. According to Lilley's final formula the noise output depends on $\int R_{22}(r, 0, 0)\,dr$ which is small compared with $\int |R_{22}(r, 0, 0)|\,dr$ because of the prolonged wavelike motion of the large eddy. However, this is an approximate formula, and a more accurate expression is obtained by using a scale based on $\int R_{22}(\mathbf{r})\,d\mathbf{V}$. The estimation of this scale would require measurement of R_{22} with separation oblique to the co-ordinate axes, and we have not yet made these measurements.

Another identification of the noise-producing part of the turbulence is Ffowcs Williams's (1963) description of it as the part convected towards the observer at the speed of sound. At jet exit Mach numbers in the subsonic range, this implies a part of the turbulence on the fringe of the probability distribution, and since the large eddies are likely to have a rather restricted range of intensities and convection velocities they should make a rather smaller than average contribution. Wills's (1963) u-component filtered space correlations at $\eta = 0$ do not noticeably demonstrate this effect, which should show up as a smaller dispersion in frequency for a given wave-number in the large-eddy range, but the large-eddy contribution to the u-component spectrum is small. The preceding argument implies that the large eddies may contribute a large part of the noise output when their convection velocity is near the ambient speed of sound, which is likely to be the case with hot choked jets. However the noise output of the large eddies may compare with that of the smaller-scale motion, the undoubted preference of the flow for a particular large eddy form seems to indicate the best method of increasing the mixing rate. As mentioned above, any increase in turbulence level (shear stress *or* intensity) is likely to increase the noise output per unit volume of turbulence so that one must choose the most efficient way of producing an increased shear stress and so reduce the total volume of noise-producing turbulence sufficiently for the *total* noise output to decrease.

The process of deducing large eddy shapes from measured correlations has been described by Grant (1958). We simply look for eddies which could generate the observed negative correlations by producing velocities of different signs at two points separated in the direction of the correlation vector. (These eddies are supposed to follow one another with random sign of rotation and with varying intensity, wavelength and position in the flow. The special property of the large eddies is that these variations of intensity, wavelength and position are sufficiently small to make the eddies detectable against the background of more

random turbulence.) For example, an eddy like a long rotating cylinder with axis in the x-direction would produce negative values of $R_{22}(0, 0, r)$ and $R_{33}(0, r, 0)$ and positive values of $R_{22}(r, 0, 0)$ and $R_{33}(r, 0, 0)$.

The correlations with noticeable negative loops in the mixing layer are $R_{22}(r, 0, 0)$, $R_{33}(r, 0, 0)$ and $R_{11}(0, 0, r)$ (figures 10, 11, 15). $R_{11}(0, r, 0)$ takes negative values near the edges of the flow, and there is a negative region in the contour plot of $R_{33}(0, r, 0)$, the most negative correlation occurring between

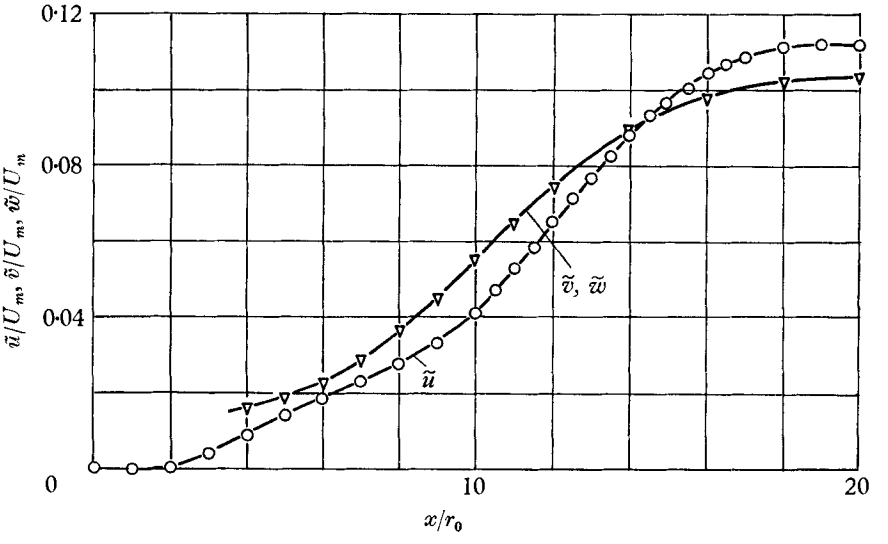

FIGURE 29. Root-mean-square turbulent intensity components $y/r_0 = 0$.

positions $y/r_0 = 0{\cdot}9$ and $y/r_0 = 1{\cdot}3$. At first sight one would guess that the $R_{33}(r, 0, 0)$ and $R_{11}(0, 0, r)$ negative loops were manifestations of an array of vortices with axes in the y-direction, probably occurring at roughly equal intervals in the x-direction. However, it appears from figures 29 and 30 that the peak in ϕ_{22}, corresponding roughly to the negative loop in $R_{22}(r, 0, 0)$, disappears by about $x/r_0 = 8$, whereas the peak in ϕ_{33} decays much more slowly. Some approximate measurements of $R_{11}(0, 0, r)$ at $x/r_0 = 8$ indicate that the negative loop in this correlation has decreased by very nearly the same factor as the peak in ϕ_{22} (or the negative loop in $R_{22}(r, 0, 0)$) at the same distance from the exit. This suggests that the negative loop in $R_{11}(0, 0, r)$ is connected with the v motion rather than the w motion. The appropriate v motion would be a mixing-jet of the type suggested by Grant, which is also suggested by the appearance of prominent diagonal streaks, apparently in the xy-plane at about $-45°$ to the axis, on the schlieren pictures (see plate 1, figure 1 (*c*)). The fluid in the mixing-jet arrives at a given point with a u-component velocity different from the mean velocity at that point because it has originated from another point in the shear layer (this is the familiar 'mixing length' argument): there is therefore a negative correlation between the u-component velocity in the mixing-jet and the u-component velocity outside the mixing-jet, particularly at points at a distance in the z-direction. We would expect the $R_{11}(0, 0, r)$ negative correlation to be more noticeable than

the $R_{11}(r,0,0)$ negative correlation because the latter is likely to be swamped by the random v-component undulations of the shear layer which produce the characteristically large scale of $R_{11}(r,0,0)$ correlations by 'shaking' the mean velocity gradient. The $R_{11}(0,0,r)$ correlation is therefore probably an indication of the presence of mixing-jets rather than vortices aligned along the y-axis. Support

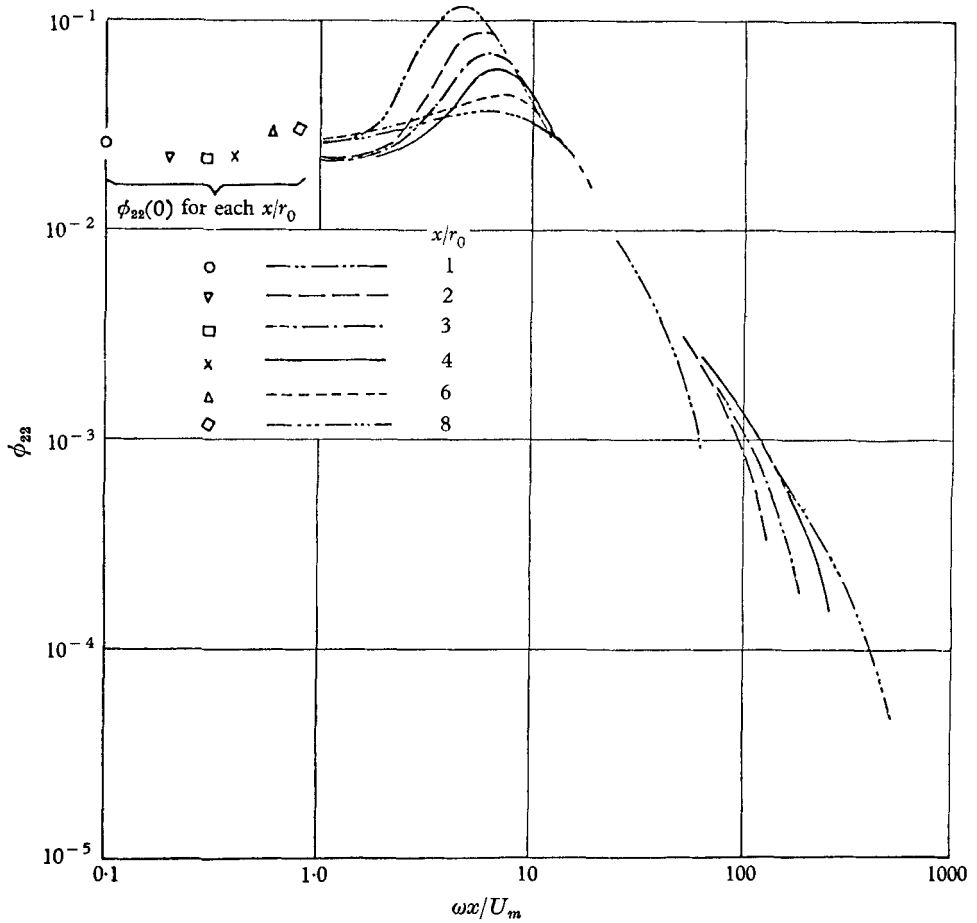

FIGURE 30. v-component spectra $y/r_0 = 1$.

for this is obtained from Grant's correlations in the wake, where $R_{11}(0,0,r)$ reaches its most negative value near the position where the mean velocity gradient is a maximum, the negative values on the centre line and near the outer edge being much smaller. In the boundary layer $R_1(0,0,r)$ also has a much more pronounced negative loop in the middle of the layer than near the surface. Grant commented that mixing-jets were indicated in the boundary layer by most of the evidence except that $R_{22}(r,0,0)$ had a single negative loop instead of being periodic. (A single negative loop usually corresponds to a wave-number spectrum without a prominent peak but still with a sharp decrease in spectral density above a certain frequency, indicating a lower bound to the eddy wavelength without a corresponding upper bound. Most spectra which fall off gradu-

ally correspond to entirely positive correlations, for example, $\phi = 2/\pi(1+\omega^2)$ and $R = e^{-t}$. There seems to be no reason why we should not imagine mixing-jets in a boundary layer (which has no point of inflexion and is therefore stable in the inviscid case) which have no preferred (eigenvalue) frequency, but which cannot survive if their size is too small. This comes to the same thing as suggesting

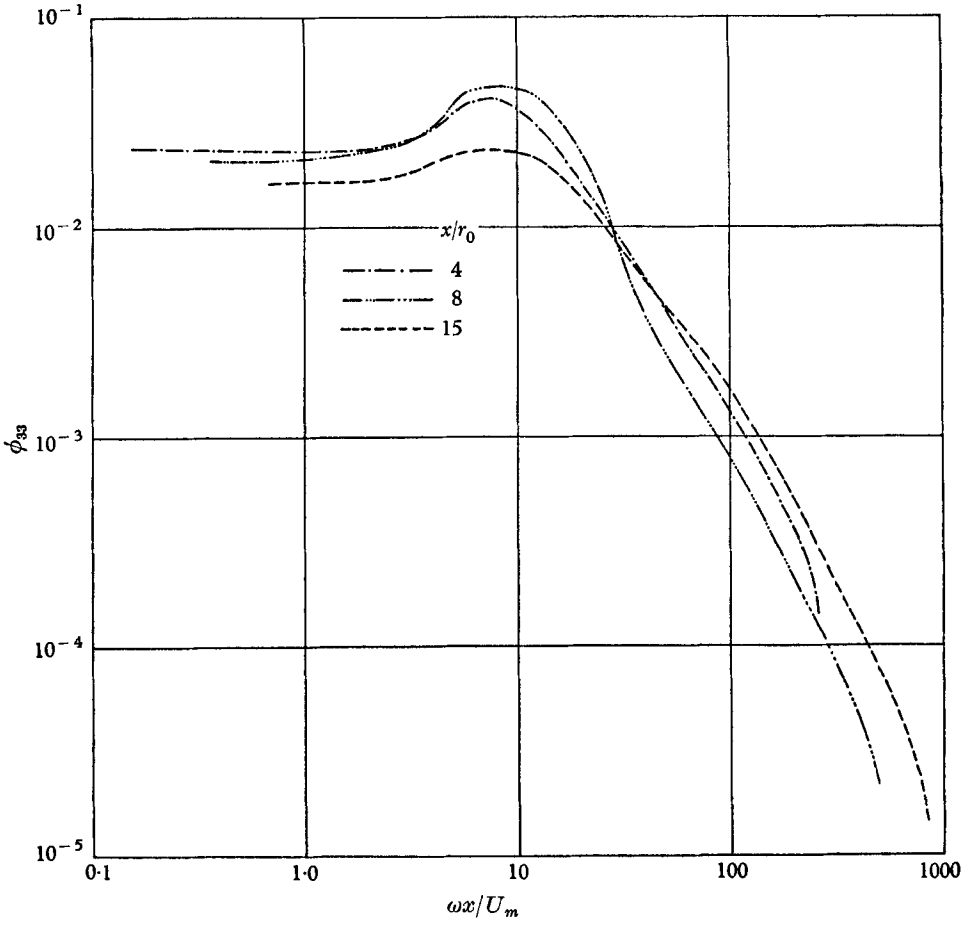

FIGURE 31. w-component spectra $y/r_0 = 1$.

that the jets follow each other at random intervals in the x-direction, with a fairly definite lower bound to the interval. There is no concrete evidence why this should be so, but the presence of an unusually sharp cut-off in the wave-number spectrum indicates some degree of organization of the eddies.)

The material part of the large eddy in the mixing layer therefore reduces to a v-component and a w-component wave motion giving rise to oscillations of $R_{22}(r, 0, 0)$ and $R_{33}(r, 0, 0)$. Although $\overline{vw}$ must be zero by symmetry, it is still possible that v and w are nearly in phase for a given large eddy and nearly in anti-phase for another so that positive and negative values of vw would cancel out. The alternative is for the v and w motions to be nearly in quadrature, leading

to an eddy like a body of fluid following a helical path with the axis at roughly $\eta = 0$. It is possible to distinguish between the alternatives by measuring $\overline{|v|\,|w|}/(\tilde{v}\tilde{w})$ or $\overline{v^2w^2}/(\overline{v^2}\,\overline{w^2})$ which would receive positive contributions from v- and w-components in phase or in anti-phase, but zero or small contributions from v- and w-components in quadrature. As a matter of convenience, $\overline{v^2w^2}/(\overline{v^2}\,\overline{w^2})$ was measured: its value for identical v- and w-components in phase or anti-phase would be equal to the value of $\overline{v^4}/(\overline{v^2})^2$ or $\overline{w^4}/(\overline{w^2})^2$, that is, about 3, whereas if v and w were in quadrature the value would be unity—at least, this is so if v can be written as $\Sigma a_n \sin(nt+\phi_n)$ and w as $\Sigma a_n \cos(nt+\phi_n)$: these are the usual Fourier representations used in (Gaussian) random noise theory but they imply the assumptions that the flatness factor is 3 and the skewness zero, and are therefore not rigorously applicable to turbulence. If $v = \sin nt$, $w = \cos nt$,

$$\overline{v^2w^2}/(\overline{v^2}\,\overline{w^2}) = \tfrac{1}{2},$$

and if v and w are completely unrelated $\overline{v^2w^2}/(\overline{v^2}\,\overline{w^2}) = 1$ again. Experimentally,

$$\overline{v^2w^2}/(\overline{v^2}\,\overline{w^2}) \simeq 2{\cdot}1$$

and for signals filtered in third-octave bands with a centre frequency at approximately the peak of the v-component spectrum $\overline{v^2w^2}/(\overline{v^2}\,\overline{w^2})$ rises to 2·7. No great accuracy is claimed for these figures which were obtained with unlinearized, unmatched X probes but they clearly support the proposition that the v- and w-components of the large eddies are in phase or anti-phase, and that the large eddy motion is predominantly a mixing-jet which, instead of moving in the xy-plane as the mixing jets in the wake appear to do, crosses the shear layer at an angle of about 45° in the yz-plane ($\tilde{v}$ and $\tilde{w}$ being approximately equal). This inclined mixing-jet also undergoes large changes in u-component velocity relative to the local mean velocity as it moves across the shear layer, and it appears from plate 1, figure 1(*c*), that the maximum rate of extension of vortex lines occurs on a line at about $-45°$ in the (x, y)-plane. This, or almost any other sort of mixing-jet structure, plausibly explains the negative areas in the contour plot of $R_{11}(0, r, 0)$.

An inclined mixing-jet of this sort could not possibly exist in isolation: it is very difficult to see how an asymmetrical w-motion of the type required could arise without some strong stimulus, and such a stimulus can only be provided by a previous mixing-jet. If we accept this last assertion, which is supported by the obvious periodicity in $R_{22}(r, 0, 0)$ and $R_{33}(r, 0, 0)$, we come to the conclusion that inclined mixing-jets follow each other at fairly regular intervals in the x-direction, and that a new jet is triggered by the preceding one at a late stage in the life of the latter: the simplest situation would be for the new jet to have the opposite sign of w-component velocity to the old jet and so—crudely speaking—tend to return along the z-axis to replace the fluid removed by the old jet. If there were only one row of mixing-jets aligned in the x-direction this would probably be the actual situation and we would have a w-motion with twice the wavelength of the v-motion. There is, however, not the slightest trace of this and we must conclude that the direction of the w-component motion is likely to be the same as that of the preceding eddy—

though over a long period of time both directions must be equally favoured. We may note parenthetically that the wave-number spectra in turbulent flow never have more than one peak: there is never any trace of a fundamental wave-number with additional harmonic components. This is a difficulty in explaining the observations in the mixing layer and the wake in terms of mixing-jets because if the jets consisted, as one would expect, of a sudden surge followed by a slower backflow, a pronounced contribution to the spectra at three times the fundamental wave-number would be present. Evidently one should not presume too much upon the degree of organization of the large eddies.

The negative region in the $R_{33}(0, r, 0)$ contour plot is consistent with the presence of inclined mixing jets. The w-motion at all negative values of η (represented in figure 14 by the sector bounded by radii from the η origin at 135 and 270 degrees to the η-axis) is well correlated. It is also *negatively* correlated with the motion near $\eta = +0{\cdot}07$, but its correlation with the motion near the outermost edge of the flow shows signs of becoming positive again. We deduce the presence of a coherent w-component motion in the regions between $\eta = 0{\cdot}3$ and $\eta = 0{\cdot}1$, which is evidently the mixing-jet at its maximum intensity. As was remarked in the discussion of the $R_{11}(0, 0, r)$ correlation, the effect of a single coherent motion in an otherwise random field is to produce an anticorrelation between points outside the area of motion and points within.

The correlations which we have not so far examined are $R_{22}(0, r, 0)$, $R_{22}(0, 0, r)$ and $R_{33}(0, 0, r)$. $R_{22}(0, r, 0)$ is everywhere positive, like $R_{ii}(r_i)$ correlations in general and the $R_{22}(0, r, 0)$ correlations in the boundary layer and wake in particular. $R_{22}(0, 0, r)$ also seems to remain positive, though a little uncertainty necessarily attaches to $(0, 0, r)$ correlations in a flow which is not accurately two-dimensional. Any sort of large eddy involving a longitudinal vortex motion would produce negative values of $R_{22}(0, 0, r)$. It is surprising that mixing-jets do not also produce negative values as was argued in the cases of $R_{11}(0, 0, r)$ and $R_{33}(0, r, 0)$, but $R_{22}(0, 0, r)$ is always positive in the wake and takes only slightly negative values in the boundary layer. If one regards Grant's argument in favour of mixing-jets in the wake as convincing, one can only accept that the jets are of sufficient extent in the z-direction for all the required v-component backflow to take place at other positions along the x-axis, although not of sufficient extent to mask the tendency for negative values of $R_{11}(0, 0, r)$ to appear. The rapid decrease in scale of $R_{22}(0, 0, r)$ as η increases is noteworthy: at $\eta = +0{\cdot}1$ it has fallen to roughly the same value as the $R_{11}(0, 0, r)$ scale. This seems to be characteristic of the inclined mixing-jets; in the wake $R_{22}(0, 0, r)$ is very nearly the same at all positions.

The negative values of $R_{33}(0, 0, r)$ found in the wake were associated with the vortex pair eddies, which also produced a periodicity in $R_{11}(0, 0, r)$ and $R_{33}(r, 0, 0)$. In the mixing layer we have no negative values of $R_{33}(0, 0, r)$, the single change of sign of $R_{11}(0, 0, r)$ can be accounted for by the mixing jets alone, and $R_{33}(r, 0, 0)$ has been shown to be closely connected with $R_{22}(r, 0, 0)$. In the wake, the negative loop in $R_{33}(r, 0, 0)$ is much less pronounced than that in $R_{22}(r, 0, 0)$ leading one to suppose that the w-component plays a less important role in the large eddy structure than the v-component. The negative values of

$R_{33}(0,0,r)$ in the wake could be explained by supposing that the w-component motion induced by the mixing-jets was a symmetrical inflow into the space left by the departing jet. In the mixing layer, however, the mixing-jets are undoubtedly asymmetrical in the (y,z)-plane, and the w-component inflow evidently tends to occur on one side only. The mixing-jets in the wake occurred alternately on either side of the centre line, so that a new jet was triggered by an old one on the other side of the wake, giving rise to a periodicity in the x-direction. The vortex pairs seem more likely to be the result, rather than the cause, of the mixing-jets, and Grant's tentative suggestion that they arose in the Kármán vortex street does not appear well substantiated—though such an origin would certainly explain the absence of any tendency to vortex pairs in the mixing layer.

We conclude, therefore, that the large eddy motion in the mixing layer consists of a series of mixing jets which, instead of lying in the (x,y)-plane as in the wake, move at an angle of about 45° to this plane. This asymmetrical motion in the yz-plane appears to be a mechanism for providing the necessary backflow: it is an alternative to the symmetrical mixing jet, with symmetrical backflow and resulting negative values of $R_{33}(0,0,r)$, found in the wake. The evidence in favour of this eddy shape is the periodicity in $R_{22}(r,0,0)$ and $R_{33}(r,0,0)$ and the close connexion between the v- and w-motions shown by the high value of $\overline{v^2w^2}/(\overline{v^2}\,\overline{w^2})$. The negative values of $R_{11}(0,0,r)$ support the suggestion of a v-component mixing-jet transferring u-component momentum across the layer, and the small negative region in the $R_{33}(0,r,0)$ contour plot suggests a coherent w-component motion in a small part of the layer.

There appears to be no law of nature determining whether the mixing-jets move inwards or outwards—in the wake of course, they move from the low-velocity, high-intensity to the high-velocity, low-intensity region—and their influence is obviously felt at both boundaries of the shear layer. There is no evidence for a simultaneous or successive departure of jets in either direction from the high-intensity region of the layer, which one would expect to produce negative values of $R_{22}(0,r,0)$. If we accept that the negative loop in $R_{11}(0,0,r)$ is caused by the mixing-jets, rather than by a rotation about the y-axis, we can deduce from the near disappearance of the negative loop at $\eta = -0{\cdot}05$ that the jet move *outwards* from $\eta > -0{\cdot}05$. The induced motion on the inner side of the shear layer should therefore be caused largely by pressure fluctuations rather than by transport of fluid from the high-intensity region, and this is compatible with the observed behaviour of the correlation length scales in this region, most of which increase as η decreases. Little can be deduced from the relative rates of spread of the boundaries: although it can be seen from figure 7 (*b*) that the rate of spread is about twice as large on the low-velocity side as on the high-velocity side, this is a direct consequence of the integral expressing conservation of momentum which, for a two-dimensional layer is $\int \eta d(U/U_m)^2 = 0$ so that the U^2 profile is roughly symmetrical about $\eta = 0$. The true centre of the layer is the high-intensity region at $\eta \simeq +0{\cdot}02$: the ratio of the inward to the outward rate of spread measured from this point is about 2:3 instead of 1:2. About all that can be said is that outward-going jets are a little more plausibly in agreement with the observed growth rate. The evidence from $R_{11}(0,0,r)$ seems to be

adequately convincing, and is supported by the observation that the u-component intensity (figure 4) is considerably less than the v- and u-component intensities near the inner edge of the layer, indicating a smaller u-component momentum transport by the mixing-jets: in the outer region $\tilde{u}/U_m$ is noticeably larger than the other two components.

Departures from self-preservation of the large eddies

For $x/r_0 > 8$ there is very little left of the v-component spectrum peak, and the w-component peak has greatly decayed by $x/r_0 = 15$. We conclude that the mixing-jets themselves die out at an early stage in the development of the asymptotic jet. Indeed we might expect that the asymmetrical mixing-jets would be rather quickly affected by curvature of the shear layer: a jet which begins by moving outward at 45° to the radius in an annular shear layer may end by moving almost radially at another point on the circumference, which is likely to disturb the triggering of a new jet by the preceding one. We have not made sufficient measurements at positions further downstream to establish the large eddy structure of the asymptotic jet but it may reasonably be assumed that such a structure does exist. Visual observations strongly suggest the presence of mixing-jets. Some ϕ_{22} and ϕ_{33} spectrum measurements at $x/r_0 = 40$ show that ϕ_{33} has a noticeable peak at all radii (though the peak frequency seems to decrease with increasing radius) but that the ϕ_{22} peak is scarcely apparent, except, of course, near the centre line where $v \equiv w$. This is in line with the observations near the end of the mixing layer region. It would indeed be surprising if the axial periodicity in the asymptotic jet were as strong as in the quasi-plane mixing layer, because of the random influence of disturbances from other parts of the circumference.

The authors wish to acknowledge the valuable advice and assistance of Dr J. A. B. Wills, and the benefit of many discussions with Dr T. H. Hodgson of the College of Aeronautics, Cranfield and Dr J. E. Ffowcs Williams. They are also grateful to Dr P. O. A. L. Davies of the University of Southampton for demonstrating the usefulness of Schlieren photography in turbulence studies, and to Mrs C. M. Stuart for help in taking figures 1 (*b*) and (*c*).

The work described in this paper forms part of the research programme carried out in the Aerodynamics Division of the National Physical Laboratory for the Ministry of Aviation. The paper is published by permission of the Director, NPL.

REFERENCES

Benney, D. J. 1961 *J. Fluid Mech.* **10**, 209.

Bradshaw, P. 1963*a* *Nat. Phys. Lab. Aero. Note* no. 1015.

Bradshaw, P. 1963*b* *Nat. Phys. Lab. Aero. Rep.* no. 1064.

Bradshaw, P. & Johnson, R. F. 1963 *Nat. Phys. Lab. Note on Appl. Sci.* no. 33.

Coles, D. 1962 In *Mécanique de la Turbulence*, Colloques Internationaux du C.N.R.S., no. 108.

Corrsin, S. & Uberoi, M. S. 1950 *Nat. Adv. Comm. Aero.* (*Wash.*), *Rep.* no. 998.

Corrsin, S. & Uberoi, M. S. 1951 *Nat. Adv. Comm. Aero* (*Wash.*), *Rep.* no. 1040.

Davies, P. O. A. L., Barratt, M. J. & Fisher, M. J. 1963 *J. Fluid Mech.* **15**, 337.

FAVRE, A., GAVIGLIO, J. J. & DUMAS, R. 1957 *J. Fluid Mech.* **2**, 313.
FISHER, M. J. & DAVIES, P. O. A. L. 1964 *J. Fluid Mech.* **18**, 97.
FFOWCS WILLIAMS, J. E. 1963 *Phil. Trans.* A, **255**, 469.
FRANKLIN, R. E. & FOXWELL, J. H. 1958 *Aero. Res. Counc.* (*London*), R. and M. no. 3161.
GRANT, H. L. 1958 *J. Fluid Mech.* **4**, 149.
JOHNSON, R. F. 1962 *Aero. Res. Counc.* (*London*), Curr. Pap. no. 685.
KISTLER, A. L. & VREBALOVICH, T. 1961 *Bull. Amer. Phys. Soc.* II, **6**, 207.
KLEBANOFF, P. S. 1955 *Nat. Adv. Comm. Aero.* (*Wash.*), *Rep.* no. 1247.
KLEBANOFF, P. S., TIDSTROM, K. D. & SARGENT, L. M. 1962 *J. Fluid Mech.* **12**, 1.
KOLMOGOROV, A. N. 1962 *J. Fluid Mech.* **13**, 82.
KOLPIN, M. A. 1964 *J. Fluid Mech.* **18**, 529.
LAURENCE, J. C. 1956 *Nat. Adv. Comm. Aero.* (*Wash.*), *Rep.* no. 1292.
LIEPMANN, H. W. & LAUFER, J. 1947 *Nat. Adv. Comm. Aero.* (*Wash.*), *Tech. Note* no. 1257.
LIGHTHILL, M. J. 1952 *Proc. Roy. Soc.* A, **211**, 364.
LIGHTHILL, M. J. 1954 *Proc. Roy. Soc.* A, **222**, 1.
LILLEY, G. M. 1958 *Aero. Res. Counc.* (*London*), *Rep.* no. 20,376.
LILLEY, G. M. & HODGSON, T. H. 1960 *AGARD Rep.* no. 276.
MAYDEW, R. C. & REED, J. F. 1963 *Amer. Inst. Aero. & Astro. J.* **1**, 1443.
MÖLLO-CHRISTENSEN, E. 1963 *Mass. Inst. Tech., Rep.* ASRL-1006.
PHILLIPS, O. M. 1955 *Proc. Camb. Phil. Soc.* **51**, 220.
RICHARDS, E. J. & FFOWCS WILLIAMS, J. E. 1959 *A.A.S.U., Rep.* no. 118.
TAYLOR, G. I. 1938 *Proc. Roy. Soc.* A, **164**, 476.
TOWNSEND, A. A. 1956 *The Structure of Turbulent Shear Flow.* Cambridge University Press.
TOWNSEND, A. A. 1958 *IUTAM Boundary Layer Research Symposium.* Berlin: Springer.
WILLS, J. A. B. 1963 *Nat. Phys. Lab. Aero., Rep.* no. 1050, and *J. Fluid Mech.* (in the press).

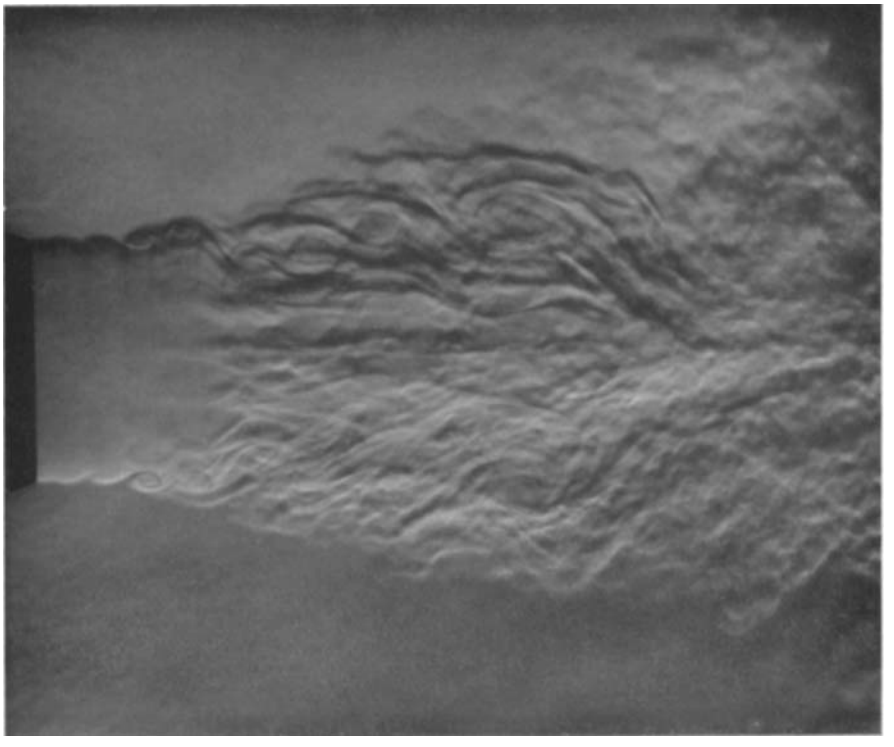

FIGURE 1 (*b*). Gas-injection schlieren pictures: 2-in. diameter jet $U_m \simeq 40$ ft./sec.

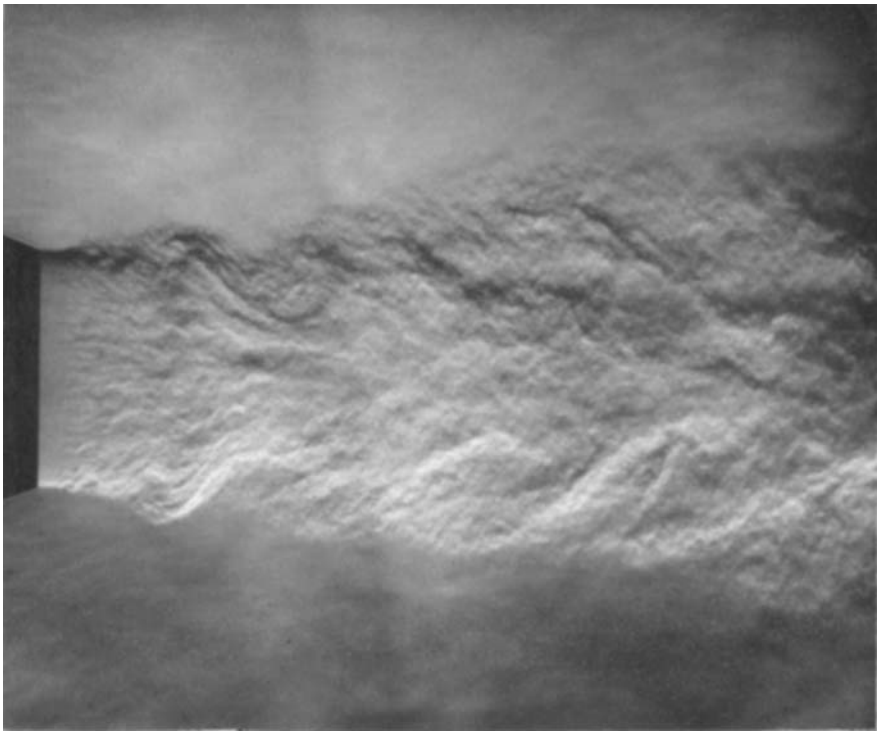

FIGURE 1 (*c*). Gas-injection schlieren pictures: 2-in. diameter jet $U_m \simeq 280$ ft./sec.